

Disaster Recovery Modeling for Multi-damage State Scenarios Across Infrastructure Sectors

by

Andrew Deelstra
Bachelor of Science, Engineer, Dordt College, 2014

A Thesis Submitted in Partial Fulfillment
of the Requirements for the Degree of

MASTER OF APPLIED SCIENCE

in the Department of Civil Engineering

© Andrew Deelstra, 2019
University of Victoria

All rights reserved. This thesis may not be reproduced in whole or in part, by photocopy or other means, without the permission of the author.

Supervisory Committee

Disaster Recovery Modeling for Multi-damage State Scenarios Across Infrastructure Sectors

by

Andrew Deelstra

Bachelor of Science, Engineer, Dordt College, 2014

Supervisory Committee

Dr. David N. Bristow, Department of Civil Engineering

Supervisor

Dr. Chris Kennedy, Department of Civil Engineering

Departmental Member

Abstract

Residents in urban areas depend on infrastructure systems to return to functionality quickly after disruptions from natural and man-made disasters to support their livelihood and well-being. This work seeks to improve the accuracy of infrastructure recovery time estimates by introducing mutually exclusive damage state modeling into the Graph Model for Operational Resilience (GMOR) and utilizing this capability for road recovery assessment in two case studies in the District of North Vancouver, British Columbia. The first case study also explores the recovery of water, wastewater, and power networks in the District, and demonstrates that power and road systems recover more slowly and are more variable in their recovery time than water distribution and wastewater collection systems. The second study specifically addresses important sections of road within the District and shows that intelligent prioritization of resource allocation for road repairs can improve recovery times by up to 37% compared to random ordering.

Table of Contents

Supervisory Committee	ii
Abstract	iii
Table of Contents	iv
List of Tables	viii
List of Figures	ix
Acknowledgments	xii
1 Introduction	1
2 Recovery from Mutually Exclusive Failure States	4
2.1 Introduction	4
2.2 Background	6
2.2.1 Dependencies	6
2.2.2 Damage States	9
2.2.3 Fragility Curves	9
2.3 GMOR Integration	10
2.3.1 Discrete and Desired Probability	14
2.3.1.1 Equations	14
2.3.1.2 Example Case	15
2.3.1.2.1 Damage State 1	16
2.3.1.2.2 Damage State 2	17
2.3.1.2.3 Damage State 3	17
2.3.1.3 Simplification for general case	18
2.3.2 Resource Prioritization	19
2.3.2.1 GMOR Conventions	20
2.3.3 Workflow	20
2.3.4 External Dependencies	20
2.3.4.1 Example	21

2.4	Conclusions.....	22
3	City-wide disaster recovery modeling of earthquake in the District of North Vancouver ...	23
3.1	Introduction.....	23
3.2	Background.....	24
3.3	Materials and Method	25
3.3.1	Study Area	26
3.3.2	Included Infrastructure Systems	28
3.3.3	System Failures and Recovery Time Parameters.....	29
3.3.3.1	Water Distribution and Wastewater Collection.....	29
3.3.3.2	Power Distribution.....	30
3.3.3.3	Road Networks	31
3.3.3.4	Sample GMOR Files	32
3.3.4	Interdependent Systems and Restoration Resources.....	32
3.4	Results and Discussion	33
3.4.1	Water Distribution	34
3.4.2	Wastewater Collection	35
3.4.3	Electric Power Distribution.....	36
3.4.4	Road Networks.....	38
3.4.5	Overall Recovery	39
3.4.6	Discussion of Results	41
3.5	Conclusion	43
4	Critical Road Network Recovery.....	44
4.1	Introduction.....	44
4.2	Background.....	47
4.3	Methodology.....	49
4.3.1	Network Creation.....	49
4.3.2	Entity Creation	52
4.3.3	Assumptions.....	52
4.4	Trials	54
4.5	Results.....	55
4.5.1	Randomized Trials	55
4.5.2	Ordered Trials	56

4.5.3	Discussion	57
4.6	Future Considerations	59
4.7	Conclusion	61
5	Conclusion and future considerations	62
Appendix A : Mutually Exclusive Failure Dependency Map Creation		69
A.1	Introduction	69
A.2	Dependency Map Creation	69
A.3	Basic Entity Structure	69
A.3.1	Duplicating Entities	70
A.3.2	Recovery Indicators	70
A.3.3	Additional Failure State	72
A.3.4	Resource Allocation	73
Appendix B : Supplemental Information for Chapter 3		74
B.1	Water Distribution and Wastewater Collection Networks	74
B.1.1	Failure and repair time distribution	74
B.1.2	Workforce resource use per repair activity	75
B.2	Water and wastewater facilities	76
B.3	Roads	76
B.4	Electricity Distribution	77
B.5	Outside scenario scope	78
Appendix C : Example GMOR files		79
C.1	Transform File	79
C.2	Scenario File	80
C.3	Order file	81
Appendix D : Maps of paths connecting origin and destination points for the road network identified in Chapter 4		82
D.1	Origin 0 – Destination 0	83
D.2	Origin 0 – Destination 1	84
D.3	Origin 1 – Destination 0	88
D.4	Origin 1 – Destination 1	89
D.5	Origin 2 – Destination 0	91
D.6	Origin 2 – Destination 1	93

Appendix E : Box plots for performance of road networks by origin-destination pair	95
Appendix F : Performance of paths for randomized and ordered trials.....	96

List of Tables

Table 1: Possible failure scenarios and repair times for the sample entity shown in Figure 2-3..	13
Table 2: Hypothetical damage state probabilities for an entity with three possible failure states	15
Table 3: Summary of repair time parameters by repair task.....	31
Table 4: Number of paths connecting indicated origin and destination points.....	52
Table 5: Mean and standard deviation of normally distributed road repair times per kilometre of road based on level of damage.....	53
Table 6: Mean and standard deviation (σ) of recovery time for origin and destination points. All values given in days.....	57

List of Figures

Figure 2-1: Example dependency map of a single entity modeled in GMOR and the functionality of the logic gates used in the model.....	8
Figure 2-2. Fragility curve for a liquid storage tank with damage states highlighted for a peak ground acceleration of 1.0 g. (European Commission 2019)	10
Figure 2-3. Dependency map for an entity with three possible damage states. The “Workforce” entity represents repair resources such as repair crews or materials. Its specifics are detailed appropriately within model scenarios to match real-world resource availability and use.	12
Figure 2-4: Tree diagram for example scenario.....	16
Figure 2-5: Operations in a facility dependent on varying levels of functionality of an incoming feeder pipe. The “I-...” entities shown here correspond to intermediary entities, such as those found in Figure 2-3, and all other dependencies are eliminated here for clarity.	21
Figure 3-1: Map of Study Area and surrounding landmarks. Background map Stamen Design, under CC BY 3.0.....	27
Figure 3-2: Path joins require a functional set of intermediate neighbourhoods to indicate recovery.....	28
Figure 3-3: Failure characterization by neighbourhood for (a) Water distribution; (b) Wastewater collection; (c) Electrical power distribution; and (d) Road and highway networks. Water and wastewater are categorized by number of breaks per neighbourhood, while power and road networks are categorized by total number of failures indicated out of 500 trials.....	33
Figure 3-4: Best, average, and worst-case scenario recovery times for the water distribution system in the District. Note that best and worst correspond to fastest and slowest overall recovery of all neighbourhoods.	35

Figure 3-5: Best, average, and worst-case scenario recovery times for the wastewater collection network in the District. Note that best and worst correspond to fastest and slowest overall recovery of all neighbourhoods. 36

Figure 3-6: Best, average, and worst-case scenario recovery times for the electric power distribution network in the District. Note the logarithmic scale on the horizontal axis and that best and worst correspond to fastest and slowest overall recovery of all neighbourhoods. As such, even though the worst-case scenario progresses more quickly than average for most of the District’s recovery, delays in later neighbourhood recovery significantly increase the overall recovery time. 37

Figure 3-7: Distribution of road network repair times for 500 trial scenarios..... 39

Figure 3-8: Average and worst-case scenario recovery time for neighbourhood road networks in the District. Note the logarithmic scale on the horizontal axis. As is also seen in Figure 3-6, the worst-case scenario for road network recovery starts off much faster than average, but significant delays near the end of the restoration period lead to a much longer overall repair time than average. 40

Figure 3-9: Overall recovery time of all systems within the District. Note the logarithmic scale on the horizontal axis, and the categorization of best and worst repair times based on the fastest and slowest repair times indicated, respectively..... 41

Figure 3-10: Box plots for (a) all studied infrastructure sectors in the district; and (b) water and wastewater systems. Note the different scales on the vertical axis of (a) and (b). The bottom and top tails of the plot represent the lowest and highest quartiles of data, respectively, while the box represents the second and third quartiles with the median indicated..... 42

Figure 4-1: Number of road segments with damage in each neighbourhood in the District of North Vancouver based on 500 trial scenarios 44

Figure 4-2: Overview of the area around Lynn Creek/Canyon and the Seymour River. Top left map shows enlarged area in the context of the whole District. The Burrard Inlet is directly south of the area shown. An overview of the surrounding area can be found in Figure 3-1..... 45

Figure 4-3: Neighbourhoods in study area with bridges highlighted. 47

Figure 4-4: Selected origin and destination points with: (a) Full road network in study area neighbourhoods; (b) Simplified road network with most dead-end and extraneous roads removed. 49

Figure 4-5: Example graph model showing nodes (circles) and edges (lines). 50

Figure 4-6: Additional road creation for roads with travel direction constraints. 51

Figure 4-7: Road repair priority levels. Origin and destination points included for reference..... 54

Figure 4-8: Distribution of recovery times for randomized prioritization..... 56

Figure 4-9: Distribution of recovery times for ordered prioritization..... 58

Acknowledgments

I would like to thank everyone who made this work possible, as well as those who made the journey to get here an enjoyable one. Special thanks to my supervisor, Dr. David Bristow, for being quick to provide answers to questions, code fixes, and thoughtful feedback throughout this process of research and writing.

Thanks also to the Cruz Lab at the Disaster Prevention Research Institute of Kyoto University for hosting me last summer and helping to develop the basis of a key part of this research.

Thank you to the E Hut crew, the VCRC community, and many other friends and family members for providing encouragement and fun along the way. You're all great.

1 Introduction

Worldwide, natural disasters affect millions of people each year and are expected to increase in severity and consequence in the future (Thomas 2017; Coppola 2006). As these increases are felt in the coming years, it is essential to recognize the strain that they place on populations and infrastructure services (Choi, Deshmukh, and Hastak 2016). A holistic understanding of disasters, their causes, and their immediate and long-term effects will help communities and organizations better prepare for the hazards that they may face.

The events and activities that surround disasters can generally be grouped into four phases: mitigation, preparedness, response, and recovery. Of these four, recovery is often regarded as the most poorly investigated and understood (Haas et al. 1977; Rodríguez, Quarantelli, and Dynes 2007; Berke, Kartez, and Wenger 1993). Much research exists surrounding the performance of systems recovery after disaster (see Bragado's (2016) study of lifeline performance after earthquakes and a book of reconstruction, restoration, and post-disaster innovation research edited by Shaw (2014), for example), but truly understanding how these systems interact and the processes that govern their recovery is often significantly more complex.

Most individuals are aware of the importance of planning for the immediate aftermath of a disaster (Donahue, Eckel, and Wilson 2014; Onuma, Joo, and Managi 2017) and trust that local and regional systems will recover in time to maintain their livelihood before their personal resources and capabilities are exhausted. Historically, however, this restoration phase was not as well planned as other phases (Haas et al. 1977), despite its critical importance in sustaining communities and supporting their ongoing development (Bristow 2019; Cassottana, Shen, and Tang 2019).

This thesis seeks to fill a gap in post-disaster restoration research by incorporating new capabilities into existing recovery modeling platforms and demonstrating the effects that disasters may have on critical infrastructure lifelines, their failure, and their subsequent return to functionality. Given the inherent unpredictability of disaster timing and magnitude, it is impossible to precisely plan for all possible situations that a region may experience. That being

said, recognizing trends and understanding recovery dynamics can inform communities and leaders to plan mitigation and response strategies that are within their control both before and in the aftermath of a disaster (Lubashevskiy, Kanno, and Furuta 2013; Rubin, Saperstein, and Barbee 1985). Doing so will increase their resilience by speeding their recovery and supporting the needs and well-being of members within their localities and organizations (Bristow 2019; Cassottana, Shen, and Tang 2019; Rodríguez, Quarantelli, and Dynes 2007).

The work presented here is separated into three chapters that expand on the concepts discussed above. Each chapter utilizes the capabilities of the Graph Model for Operational Resilience (GMOR), a computational engine used to model the recovery of infrastructure and organizational systems after failure due to disaster (Bristow and Hay 2017; Bristow 2019). GMOR is intended for use as a planning tool to help stakeholders and organizations understand the effects of disasters on the functionality and recovery of systems within their communities. The specifics of GMOR's integration are addressed in detail within each chapter and examples are included to illustrate key points.

The first chapter (Chapter 2) describes a new methodology for incorporating differing levels of component damage into GMOR models. This process allows for the failure of physical systems (such as roads, pipelines, or tanks) to be more accurately represented in GMOR models to improve estimates of required recovery time.

Chapter 3¹ details a case study of the recovery modeling of various infrastructure systems within the District of North Vancouver at a neighbourhood level. An assessment was previously conducted by the district for a hypothetical earthquake scenario, and data gathered from the assessment was used to perform the study in this chapter. The systems modeled include water distribution, wastewater collection, electrical power transmission, and road and highway transportation. My contributions to this work were to revise the model by incorporating my new

¹ This chapter was written with Dr. David Bristow and submitted to the International Journal of Disaster Risk Science (IJDRS) on May 31, 2019, for a special issue on data driven approaches for integrated disaster risk management and is currently undergoing review. It has been edited from its submitted form to better fit within the broader context of this thesis.

methodology from Chapter 2, running simulations, analyzing results and leading the writing of the chapter.

Chapter 4 demonstrates the process of recovery for an important group of roads in the District of North Vancouver. These roads are critical for connecting various sections of the District, and their recovery facilitates the movement of goods and services throughout the area. Specific paths within the area are considered to best illustrate the process of recovery.

Finally, a conclusion is offered that summarizes key points and lessons learned throughout the previous chapters. It also presents considerations for future work and goals for ongoing improvements within GMOR and the field of resilience and recovery modeling as a whole.

2 Recovery from Mutually Exclusive Failure States

2.1 Introduction

Natural hazards and malicious attacks threaten critical infrastructure systems throughout the world. The ability of these systems to recover quickly after failure is essential for their ongoing operation and support of the communities that surround them. Modeling this recovery can help policy-makers and operators develop plans to minimize loss when destructive scenarios occur, thus increasing the resilience of the communities that they serve (Bristow 2019; Cassottana, Shen, and Tang 2019; Rodríguez, Quarantelli, and Dynes 2007).

Ensuring the accuracy of the models used to represent and test infrastructure systems and their exposure to disaster is essential for informing communities about the hazards and risks that they face. Various approaches exist for modeling disaster scenarios, each with its own strengths, required inputs, and priorities. Some focus on the immediate effects of a disaster and provide estimates of damages to affected systems and components, while others deal with recovery processes related to these damaged systems. The work presented here relates to the interaction between these two areas of research and expands on recovery modeling processes to more accurately align them with damage estimates. Better representation of damages enables more detailed estimates of recovery times, which informs reconstruction activities and resources.

One tool commonly used in this field is Hazus, developed by the US Federal Emergency Management Agency (FEMA) for estimating loss and damages due to hypothetical earthquakes and other hazards. The software includes regional parameters for locations in the United States and incorporates demographic and infrastructure data for the represented areas. Hazus draws from a large database of past hazards and expert knowledge in order to predict damages due to the defined hazard. Based on these predicted damages, Hazus then produces an estimate of economic losses and system recovery time for the affected area (FEMA 2011).

Since the data that Hazus uses for recovery time is based primarily on previous hazards and expert judgement, there is a great deal of uncertainty in the results that are produced. This uncertainty is one of the primary motivations for the development of more accurate recovery models such as the one presented here.

The Graph Model for Operational Resilience (GMOR. Bristow and Hay 2017; Bristow 2019) is a modeling framework that attempts to provide an understanding of uncertainty related to infrastructure system recovery time. Rather than using aggregate data for estimating recovery, GMOR instead focuses on the recovery of individual system components and tracks how these components interact with and relate to one another (Bristow and Hay 2017). For example, where Hazus assesses a power system and reports a probability of recovery after a certain time for each component, GMOR instead tracks the functionality of each component and models how they relate to and are dependent on other systems over time as recovery progresses. Historical data is used in both cases, but the goal of GMOR is to increase the level of detail of the data used and the reported results so that individual component recovery can be tracked alongside overall system recovery.

The objective of the work presented in this chapter is to further improve the interaction of models developed in GMOR with other assessment tools and give users better insight into how systems respond to damage and recover over time. This is accomplished by developing a methodology by which multiple possible levels (or types) of damage for individual components may be modeled. For each damage state, a unique required repair time is specified to more accurately represent the loss from the type of damage sustained. Because many tools that produce damage estimates (such as Hazus) indicate the probability that systems or components will experience any given level of failure, this methodology improves GMOR's compatibility with a wide range of such tools.

The chapter proceeds as follows. First, a discussion of dependencies and how they are developed and used in GMOR models is presented in Sections 2.2 and 2.2.1. Next, an introduction to damage states and fragility curves is offered in Sections 2.2.2 and 2.2.3. In section 2.3, the integration of GMOR with the multiple failure level methodology is detailed, including the logic and mathematical processes used in the updated models.

It is important to note that much of the work presented in this chapter is theoretical, with example cases scattered throughout to illustrate key concepts. Broader case studies are included in Chapters 3 and 4 and provide additional details and process descriptions for the use of this methodology in assessing the recovery of a road network in the District of North Vancouver after a modeled magnitude 7.3 earthquake.

2.2 Background

Certain components within an infrastructure system may be damaged to varying levels. The ability to properly model the damage is critical in order to provide an accurate representation of recovery time, especially when downstream dependencies may be affected by the failure. Examples of components that may be affected by this type of damage behaviour include tanks, pipes, and transportation systems. The so-called mutually exclusive nature of the damage indicates that only one failure can occur at a time for a given component. For example, a tank cannot be only slightly buckled and demolished by an explosion at the same time. Pipes, roadways, and other linear infrastructure systems are often split into sections to allow for various levels of damage to be represented along their lengths. These lengths are joined to one another and to other infrastructure systems within a model to form interconnected networks of dependencies. When small sections fail, the network fails as a result of these dependencies. Only when each section is recovered can the full network recover as well.

2.2.1 Dependencies

In GMOR models, dependencies are defined within infrastructure systems. These dependencies include entities that represent resources, times, and processes required for a system component to function effectively. These entities may in turn depend on others within the system, leading to a network of connected components and processes in a model. When a GMOR model is run, its dependencies are placed in a network and resources are allocated to track the recovery of a system when subject to a set of failures.

An example of a basic entity structure with dependencies (referred to as a “dependency map”) is shown in Figure 2-1 alongside the symbols for the logic gates used in GMOR models. Dependencies are represented by directed lines – entities at the tip of the arrow are dependent on those at the base of the line. Entities that are self-dependent (those with a directed line leaving and re-entering without passing through another entity) are required for the model to run by triggering an initial positive state value that other entities in turn depend on. The self-dependencies also establish the initial state value (by means of a stored parameter value) for entities whose initial states are determined probabilistically (such as failure entities discussed in later sections).

Within these models, a 1 indicates that an event has occurred or a component is functional, whereas a 0 indicates that an event has not occurred or a component is non-functional. Following the logic gates for the entity in Figure 2-1, it can be seen that when a failure does not occur (takes a value of 0), the entity holds a value of 1, indicating that it has not lost any functionality. If a failure does occur, however, the failure takes on a value of 1 and the entity takes a value of 0 initially. The resource entity must then be utilized in order to restore the entity to full functionality. The resource is allocated for a certain amount of time specified in the repair time entity. This repair time introduces a delay in the model such that the overall entity is only shown as fully functional once the specified repair time has passed. This basic structure is replicated and utilized repeatedly to form increasingly complex GMOR models.

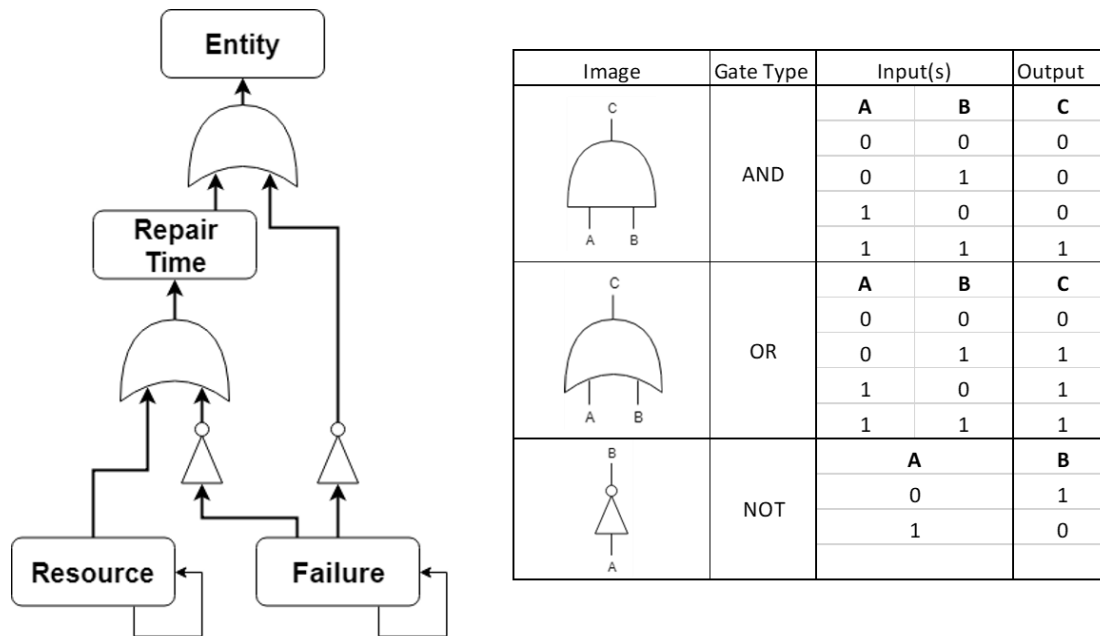


Figure 2-1: Example dependency map of a single entity modeled in GMOR and the functionality of the logic gates used in the model.

Note that the diagram shown in Figure 2-1 only shows the names and dependencies of entities within a GMOR model. Other entity parameters such as probability of occurrence, geospatial location, and restoration time are included in models but not shown here.

The key parameter used for recovery assessment in GMOR is the repair time of each component or process. In previous models built in GMOR, entities only failed in a single way. That is, an entity could be either functional or non-functional, with no distinction made for level of damage or how that might impact the entity's required repair time.

As mentioned previously, Hazus does not track dependencies of individual components or interconnected systems. The dependencies are essentially built in to the whole system or facility of interest. For example, if a Hazus model shows that a factory takes a certain amount of time to recover, the lifeline systems and processes that the factory depends on are assumed to have been repaired within that timeframe. No specific connection to those lifelines or processes is made within the model, so delays in repairs to those systems would not be represented in the recovery time of the factory.

2.2.2 Damage States

While Hazus does not track recovery in a detailed manner, its documentation does include comprehensive information related to damage states resulting from natural hazards (FEMA 2011). Damage states are a numerical representation of the level of failure of a specific component. For a liquid storage tank, for example, Damage State 1 (DS-1) represents no damage, states 2-4 represent varying levels of failure and some release of tank contents, and DS-5 represents total tank collapse and complete loss of contents (American Lifelines Alliance 2001).

Each of these levels of failure requires a different repair time that increases as the level of damage increases. This is not only apparent intuitively, but it is also supported by studies of previous natural disasters, such as the Applied Technology Council's evaluation of earthquake damage in California (Applied Technology Council 1985). Further, differing failure levels may require different resources for recovery, such as specialized repair crews or tools, though these are not discussed or modeled for the purposes of this chapter.

2.2.3 Fragility Curves

Fragility curves are used to establish the probability of a given damage state occurring in a given component category based on a given type of hazard. An example fragility curve gathered from the Joint Research Centre's RAPID-N "Rapid Natech Risk Assessment Tool" is shown in Figure 2-2. This tool includes numerous fragility curves for a variety of industrial components and allows users to generate ground motion and failure data for potential earthquake scenarios anywhere in the world (European Commission 2019). This fragility curve represents the effects of an earthquake on a liquid storage tank. The scale on the horizontal axis represents the severity of the hazard – in this case, the peak ground acceleration (PGA, commonly measured in units of g – acceleration due to gravity on Earth) of an earthquake at the location of the tank.

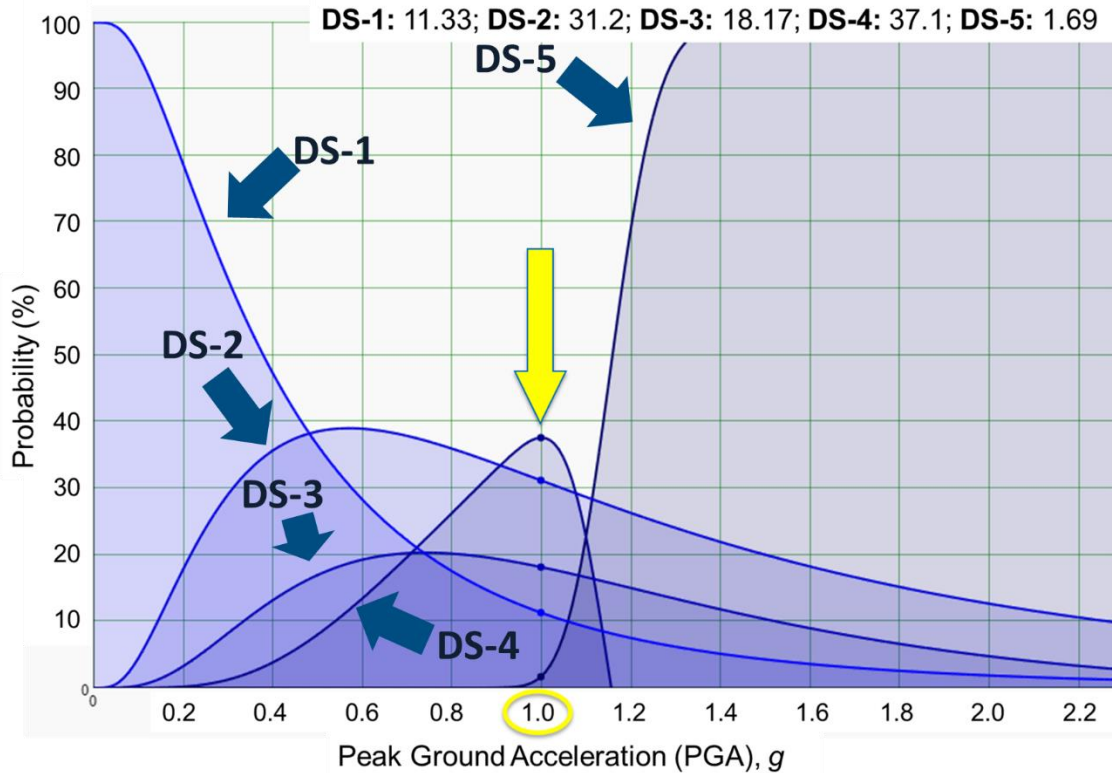


Figure 2-2. Fragility curve for a liquid storage tank with damage states highlighted for a peak ground acceleration of 1.0 g. (European Commission 2019)

The vertical axis commonly shows either the discrete or cumulative probability of each possible damage state based on a specified PGA. In this case, the discrete probability is shown. That is, if the predicted PGA is 1.0g at the location of a tank of interest, the probability of the tank being damaged to a level of DS-1 is 11.33%, DS-2 is 31.2%, and so forth. These values are indicated numerically at the top of the figure, and serve as input parameters for multiple-damage state models in GMOR.

2.3 GMOR Integration

In the following sections, a generic entity with three possible damage states is used to illustrate the process of creating models in GMOR that allow for the simulation of mutually exclusive failure states.

A dependency map for the entity is shown in Figure 2-3. For reference, logic gates and symbols used in Figure 2-3 are indicated on the right side of Figure 2-1 and a step-by-step explanation of the process of generating this dependency map is given in Appendix A. Names of entities within the model are bolded throughout this section to ease their identification.

The full dependency map represents each of the different entities required to keep the example **Entity** operational. As shown, **Entity** depends on **End Repair of Entity** which is in turn dependent on three additional entities, **Indicator 1**, **Indicator 2**, and **Indicator 3**. The indicator entities are implemented with no functionality on their own, but serve as indicators of the status of failure and recovery entities.

In the model shown in Figure 2-3, the **Indicator** entities and **Repair time for...** entities are initialized with a value of 0. In addition, a failure entity with a state value of 1 indicates that a failure has occurred. For example, the **Indicator 1** entity depends on NOT **DS-1 Failure** OR **Repair Time for DS-1**. If the state value of **DS-1 Failure** is 0, **Indicator 1** is immediately functional and requires no additional repair or resources. If, however, the state value of **DS-1 Failure** is 1, the OR gate dictates that **Repair Time for DS-1** must take on a value of 1 for **Indicator 1** to function.

In order for **Repair Time for DS-1** to take on a value of 1, **Workforce** must be utilized (through **Initiate Repair of Entity**) and the repair time will switch from a 0 to a 1 after a given amount of time specified in the **Repair Time for DS-1** entity. The **Initiate Repair of Entity** and **End Repair of Entity** entities allow GMOR to prioritize the allocation of resources for multiple components within a model that share a limited resource. This allocation can be user-defined or randomized and is described further in Section 2.3.2.

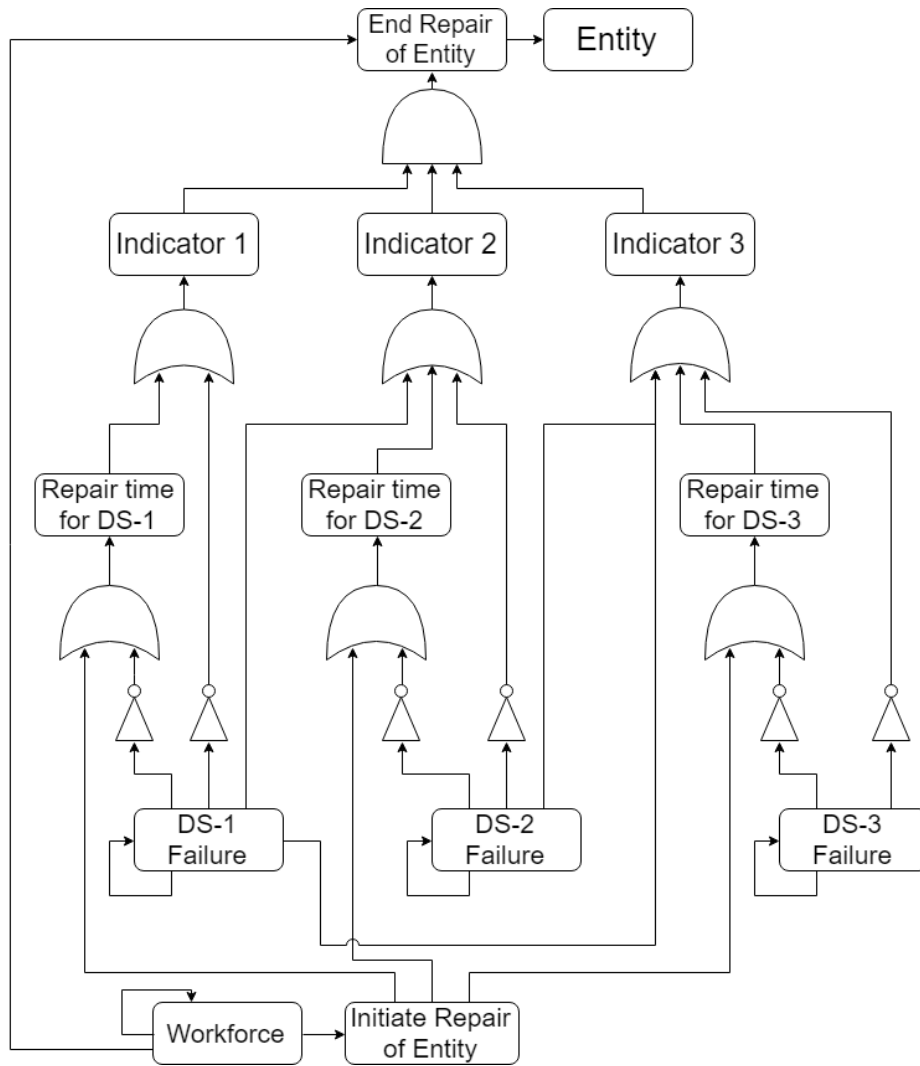


Figure 2-3. Dependency map for an entity with three possible damage states. The “Workforce” entity represents repair resources such as repair crews or materials. Its specifics are detailed appropriately within model scenarios to match real-world resource availability and use.

With that logic in mind, a table with possible initial state combinations for failures and the selection of required repair times for these combinations is shown in Table 1. An explanation of key points is offered in the following paragraphs. Note that even though damage states are by definition mutually exclusive, Table 1 indicates that a number of failure entities may take on an initial value of 1 in a modeled scenario. The rationale for these situations is described in following sections.

Table 1: Possible failure scenarios and repair times for the sample entity shown in Figure 2-3.

Scenario	Failure (initial parameter value in model):			Initial value of indicator entities:			Realized failure/ required repair time
	DS-1	DS-2	DS-3	Ind. 1	Ind. 2	Ind. 3	
1	0	0	0	1	1	1	N/A
2	0	0	1	1	1	0	DS-3
3	0	1	0	1	0	1	DS-2
4	0	1	1	1	0	1	DS-2
5	1	0	0	0	1	1	DS-1
6	1	0	1	0	1	1	DS-1
7	1	1	0	0	1	1	DS-1
8	1	1	1	0	1	1	DS-1

The realized failure and required repair time indicated in the rightmost column is used by GMOR in processing a given scenario. Based on the scenarios indicated in Table 1, it can be seen that failures are realized in ascending order. That is, the first failure state (lowest DS number) that has a value of 1 is the one whose repair time is used for the recovery of **Entity**. Note in Scenarios 3 and 4, for example, that **Repair Time of DS-2** is the overall repair time, even though in Scenario 4, both **DS-2 Failure** and **DS-3 Failure** have an initial state value of 1. This is confirmed by following the logic in Figure 2-3, where a value of 1 for **DS-2 Failure** will pass a value of 1 to **Indicator 3**. As a result, the repair time entity associated with **Indicator 3 (Repair Time for DS-3)** is not required for the recovery of **Entity** to occur. This leads to the conclusion that in every scenario, only one indicator entity has an initialized value of 0. The indicator that holds the 0 corresponds to the realized failure and its associated repair time.

2.3.1 Discrete and Desired Probability

GMOR allows the likelihood of failure for a specific entity to be defined probabilistically. This functionality may also be used to model various levels of failure of a single entity, such as the damage states described above. However, simply using discrete probabilities for each possible damage state would not yield proper results. Since each failure has a discrete probability of occurrence of less than one, a no-failure situation could be modeled. DS-1 already indicates that no failure has occurred, so this would lead to inaccurate results. Additionally, based on the logic shown in the dependency map in Figure 2-3 (where the first indicated failure dictates the recovery time), lower level failures would be disproportionately represented in the modeled scenarios.

To prevent this overrepresentation and develop an accurate distribution of failure scenarios, conditional probabilities are used. Simply put, conditional probabilities take into consideration the fact that more than one condition may need to be met for a desired situation to occur. For example, in the fragility curve shown in Figure 2-2, the discrete probability of DS-3 occurring is approximately 18% at a peak ground acceleration of 1g. Given the information in Table 1, however, DS-3 can only be the realized failure in the model if both DS-1 and DS-2 have not occurred. Conditional probability equations offer a solution in which these additional constraints (DS-1 and DS-2 must not occur) are respected so that DS-3 will be the realized failure in 18% of all cases. The equations used to establish these conditional probabilities are illustrated in the following section.

2.3.1.1 Equations

By the Kolmogorov definition, the conditional probability of an event A occurring given that an event B has occurred is given by the following equation (Kolmogorov and Bharucha-Reid 1956):

$$P(A|B) = \frac{P(A \cap B)}{P(B)} \quad (1)$$

In this equation, $P(A \cap B)$ is the probability that both event A AND event B occur.

2.3.1.2 Example Case

As an example scenario, an entity (such as a road or liquid storage tank) with three possible damage states is exposed to a certain natural hazard. A fragility curve for the entity and hazard is consulted, and discrete probabilities are taken from the curve and recorded in Table 2. Because at least one of these damage states must occur in any scenario, the values of their probabilities sum to one.

Table 2: Hypothetical damage state probabilities for an entity with three possible failure states

Damage State	Probability
DS1	0.5
DS2	0.3
DS3	0.2

In this example, probability of occurrence for a given damage state is represented as $P(x)$, where x represents the scenario of interest. Overlined values indicate that an event has not occurred. For example, $P(\overline{DS1})$ is the probability that $DS1$ has not occurred and is equal to $1 - P(DS1)$. In many of the following equations, the probability of multiple damage states not occurring is considered and is shown, for example, as $P(\overline{DS1} \cap \overline{DS2})$. This is the probability that neither $DS1$ nor $DS2$ has occurred and is calculated as:

$$P(\overline{DS1} \cap \overline{DS2}) = 1 - (P(DS1) + P(DS2)) = 1 - P(DS1) - P(DS2) \quad (2)$$

Hyphens that are normally shown in damage state numbers are eliminated here ($DS-1$ becomes $DS1$ for example) to provide clarity and prevent confusion between these hyphens and those used for subtraction. Asterisks (*) indicate a calculated conditional probability that is subsequently used in a GMOR model. For example, the probability of occurrence for $DS2$ as indicated in a fragility curve is represented as $P(DS2)$, whereas the probability used in the model is shown as $P(DS2^*)$.

A visual representation of the values included in Table 2 is shown in a tree diagram in Figure 2-4. Again, overlined numbers indicate that the damage state represented by that number has not occurred. Only three positive values (indicating the probability of occurrence) are shown on the right side of the diagram, indicating that each damage state can occur if and only if the other two do not occur.

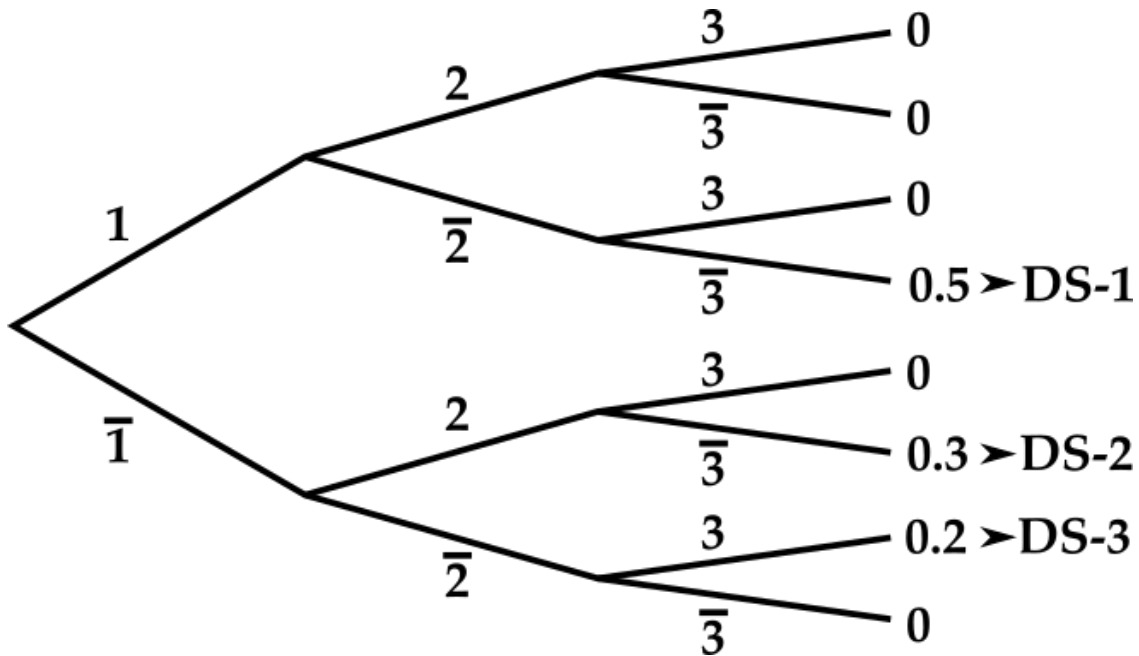


Figure 2-4: Tree diagram for example scenario

2.3.1.2.1 Damage State 1

The discrete probability of occurrence of damage state 1 ($DS1$) is given as 0.5 in Table 2. By the logic shown in Figure 2-3 and Figure 2-4, this probability is completely independent of the probability of occurrence of the other two damage states. That is, if $DS1$ shows a state value of 1, it will occur with no dependence on the states of the other two failure entities are. Therefore:

$$P(DS1^*) = P(DS1) = 0.5 \quad (3)$$

2.3.1.2.2 Damage State 2

The discrete probability of occurrence of damage state 2 ($DS2$) is given as 0.3 and is dependent on $DS1$ not occurring. The conditional probability equation is set up as follows:

$$P(DS2^*) = P(DS2|\overline{DS1}) \quad (4)$$

Where, from Equation 1:

$$P(DS2^*) = P(DS2|\overline{DS1}) = \frac{P(DS2 \cap \overline{DS1})}{P(\overline{DS1})} \quad (5)$$

On the left side of Equation 5 is the conditional probability value that will be calculated and used in GMOR. On the far right are known values used to make that calculation. $P(DS2 \cap \overline{DS1})$ can be read as the probability of $DS2$ occurring when $DS1$ has not occurred. This value is given in Table 2 as a probability of 0.3. Again, the occurrence of the higher-level failure ($DS3$) has no bearing on the occurrence of $DS2$ because:

$$P(DS2 \cap \overline{DS1}) = P(DS2 \cap \overline{DS1} \cap DS3) + P(DS2 \cap \overline{DS1} \cap \overline{DS3}) = 0 + 0.3 \quad (6)$$

The values in Equation 6 can be confirmed by following the branches of the tree diagram in Figure 2-4. Equation 5 then becomes:

$$P(DS2^*) = \frac{0.3}{1 - P(DS1)} = \frac{0.3}{0.5} = 0.6 \quad (7)$$

2.3.1.2.3 Damage State 3

The discrete probability of occurrence of damage state 3 ($DS3$) is given as 0.2 and is dependent on both $DS1$ and $DS2$ not occurring. The conditional probability equation is developed as shown:

$$P(DS3^*) = P(DS3|\overline{DS1} \cap \overline{DS2}) \quad (8)$$

where

$$P(DS3|\overline{DS1} \cap \overline{DS2}) = \frac{P(DS3 \cap \overline{DS1} \cap \overline{DS2})}{P(\overline{DS1} \cap \overline{DS2})} \quad (9)$$

Again, the numerator of the right side of Equation 9 is equal to the given probability of 0.2. The denominator is read as the probability of both $DS1$ and $DS2$ not occurring. From Equation 2, this gives:

$$P(\overline{DS1} \cap \overline{DS2}) = 1 - P(DS1) - P(DS2) \quad (10)$$

$$1 - P(DS1) - P(DS2) = 1 - 0.5 - 0.3 = 0.2 \quad (11)$$

which then gives

$$P(DS3^*) = P(DS3|\overline{DS1} \cap \overline{DS2}) = \frac{0.2}{0.2} = 1 \quad (12)$$

It may seem odd at first that the conditional probability of occurrence for $DS3$ is calculated as 1, but given a situation in which both $DS1$ and $DS2$ do not occur, $DS3$ must occur. If it did not, the failures may all have a state value of 0, which, as indicated in Section 2.3.1 is not possible.

Given this information, it can now be shown that Scenarios 1, 3, 5, and 7 in Table 1 can never occur in a model using this probability formulation. In each of these scenarios, Failure of Entity DS-3 is assigned a value of 0, which is impossible because its probability of occurrence in the model will always be indicated as 1.

2.3.1.3 Simplification for general case

The results from the exercise above can be expanded for a four-failure state entity and summarized as follows:

$$P(DS1^*) = P(DS1) \quad (13)$$

$$P(DS2^*) = \frac{P(DS2)}{1 - P(DS1)} \quad (14)$$

$$P(DS3^*) = \frac{P(DS3)}{1 - P(DS1) - P(DS2)} \quad (15)$$

$$P(DS4^*) = \frac{P(DS4)}{1 - P(DS1) - P(DS2) - P(DS1)} \quad (16)$$

For a general case with N possible damage states, the first damage state is given as:

$$P(DS1^*) = P(DS1) \quad (17)$$

And for the i^{th} failure state:

$$P(N_i^*) = \frac{P(N_i)}{1 - P(N_{i-1}) - P(N_{i-2}) - \dots - P(N_1)}, i > 1 \quad (18)$$

The results of this calculation are used to define the probability of occurrence for mutually exclusive damage states in GMOR models that follow the structure shown in Figure 2-3.

2.3.2 Resource Prioritization

Within the GMOR framework, functional entities (such as tanks or pipelines) are ultimately dependent on resources. For the entity shown in Figure 2-3, for example, each indicator has a unique repair time associated with it. Each of the repair time entities, however, is connected to the same resource via the “Initiate Repair of Entity” entity. The resource listed in this example is labeled simply as “Resource”, and only the single overall component (“Entity”) is dependent on it. In a larger system, however, multiple components may depend on the same resource. Resources in GMOR can be representative of specialized repair crews, specific tools, or general labour requirements.

In practice, resources are limited in their supply and must be distributed to areas where they are needed. Ideally, this distribution would occur in an order that most effectively reduces recovery times for critical components. However, that order is not likely known, especially in the critical hours that immediately follow a natural disaster (Lubashevskiy, Kanno, and Furuta 2013).

GMOR allows for the order of recovery resource allocation for entities to be specifically defined in models to assess how the order of resource distribution affects recovery time. If no order is specified, GMOR will assign values randomly. Section 4.5 offers an example of the improvement that can be seen by prioritizing resources for recovery.

Recovery time is not the only important factor to consider when establishing resource prioritization, however. Users may be more concerned about the recovery of a specific entity than about how long it takes for a whole system to recover. For example, a wastewater treatment plant may want to prioritize repairing leaks in chemical storage tanks before fixing a collapsed water tank.

2.3.2.1 GMOR Conventions

Resource prioritization in GMOR is done by assigning numerical value to an Initiate Repair entity associated with a given resource in a model. The lower the assigned number, the higher the priority. If the values for two or more entities are equal, GMOR will randomly assign an order for prioritization. The values are stored in a database that is read by GMOR while a model is being compiled and run.

2.3.3 Workflow

Working with GMOR involves the creation of entities that represent physical objects, systems, or organizational structures in a model, then generating dependencies (indicator, repair time, resource, and failure entities, for example) for each of those entities. Parameter values such as repair time and probability of failure are then added to their respective parts of the model and an order is specified (or left to GMOR to determine randomly) for resource allocation.

2.3.4 External Dependencies

As mentioned in Section 2.3, the indicator entities shown in Figure 2-3 serve no direct purpose for providing functionality to any other entity. They do, however, quickly indicate the level of failure that an entity has experienced. This indication can be useful for external services that may be dependent on an entity for a certain level of functionality. For example, a facility may require an incoming pipe to provide fuel for its operations. The facility would still function if the pipe is undamaged (DS-1) or only slightly damaged (DS-2), but could not continue its operations if the pipe is completely collapsed (DS-5). An example is included below to illustrate this process and could be extended to multiple functions reliant on the same component.

2.3.4.1 Example

A pipe (Pipe-1) with four possible damage states feeds into a facility – in this case, DS-4 represents total failure, while DS-1 represents no damage, DS-2 represents slight damage, and DS-3 represents moderate damage. Within this facility are two functions (Operation-1 and Operation-2) that require the pipe for them to function properly. Operation-1 can run on a limited supply from the pipe, so it is only incapacitated if the pipe is moderately or completely damaged (DS-3 or DS-4). Operation-2, however, requires a higher supply from the pipe, so it can only function if the pipe is undamaged (DS-1).

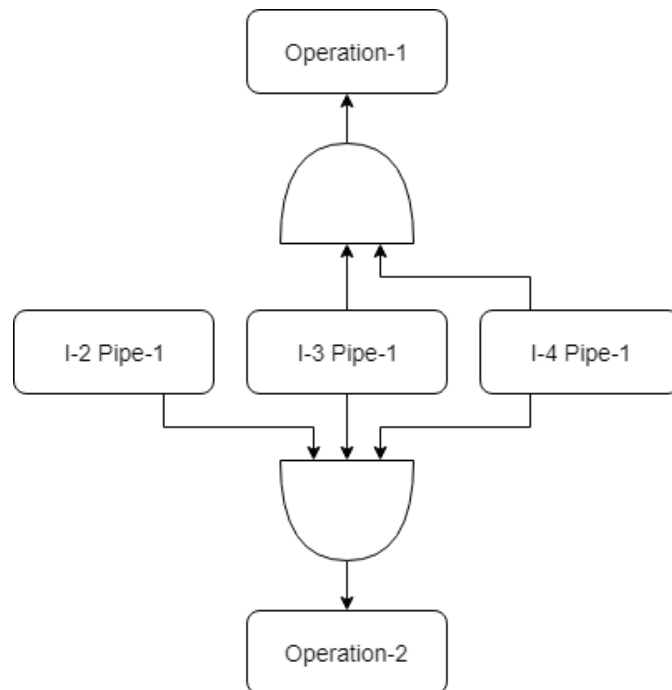


Figure 2-5: Operations in a facility dependent on varying levels of functionality of an incoming feeder pipe. The “I-...” entities shown here correspond to intermediary entities, such as those found in Figure 2-3, and all other dependencies are eliminated here for clarity.

A dependency map for the pipe and operations is shown in Figure 2-5 to illustrate the situation described above. Note that this figure only includes the intermediary entities for the pipe and names of the operations. Failure, repair time, and resource entities for both operations and the pipe are not shown here for simplicity.

One important caveat to note in this methodology is the assumption that there are no interruptions in service for the affected entity. In the above example, for instance, even though DS-1 indicates a lack of failure, a facility operator would likely not know that the pipe is undamaged immediately after a disaster. They may choose to suspend processes to perform equipment inspections, in which case the pipe could be shut off even though it has not experienced a failure. This would result in the physical operation not being accurately represented in the modeled operation. Other cases, such as those representing road damage, may be better suited for implementing this functionality and are discussed in Section 4.6.

2.4 Conclusions

The multiple-damage state methodology provides new capabilities for modeling complex systems in GMOR. These capabilities can be used in computational models to more accurately represent critical components, the ways in which they fail, and the resources that they need to recover. In addition, this methodology provides more opportunities for GMOR inputs to integrate with outputs from other damage estimation tools. Producing more accurate models can help better inform decision makers and planners when it comes to implementing systems to prepare for disaster and subsequent recovery to improve outcomes for businesses, citizens, and communities.

3 City-wide disaster recovery modeling of earthquake in the District of North Vancouver

3.1 Introduction

Critical infrastructure lifelines, such as electrical power, water and wastewater systems, and road networks, are essential for supporting the continued functioning of communities, and are closely linked to the stability of urban populations (Ouyang 2014; Bristow 2019). As such, damage to these lifelines due to a disaster or malicious attack can have a profound impact on the wellbeing and livelihood of residents in urban areas. Increasingly complex infrastructure networks lead to interdependencies between systems that are challenging to assess (Loggins and Wallace 2015). To prevent the propagation of failures within and between systems in a disaster setting, these interdependencies must be identified and protected.

The stages of disaster risk management can be generally grouped into four phases, including mitigation, preparedness, response, and recovery (Berke, Kartez, and Wenger 1993; Rubin, Saperstein, and Barbee 1985). Of these four, recovery is often regarded as the most poorly understood and researched (Rodríguez, Donner, and Trainor 2018). Given that a key component of resilience is a timely return to pre-disaster (Haines 2009), or even superior conditions, recovery and resilience are closely linked concepts and should be considered concurrently in developing urban infrastructure protection processes.

Many nations develop plans that identify, classify, and establish strategies for the protection and continued operation of their infrastructure systems. These plans, while necessary for promoting unified goals, standards, and requirements at a national scale, do not address specific issues that are experienced within individual communities. As such, they should encourage plans for protection that are made at regional and local scales (Rodríguez, Donner, and Trainor 2018). The variation in population, needs, and concerns of dissimilar urban areas require individual infrastructure protection assessment to provide value within the local context (Bristow 2019). Individuals can play a role in protecting their own homes and livelihoods, but

must also trust that broader infrastructure systems will be in place within a reasonable amount of time to continue to support their recovery in the aftermath of a disaster (Onuma, Joo, and Managi 2017).

The objective of this paper is to demonstrate data-driven modeled estimates of multi-infrastructure restoration at the city-wide scale. Features from existing resilience and recovery tools are used to provide a novel assessment methodology that integrates probable damage, restoration priority, and dependencies within systems to illustrate the dynamics of urban recovery. In the sections that follow, hazard assessment tools are introduced, a study area, infrastructure systems, and hypothetical hazard are defined, and trial results are presented with key findings and suggestions for future research highlighted.

3.2 Background

Various data-driven methodologies exist for the purposes of hazard assessment and recovery modeling that serve a wide variety of needs. Researchers such as Miles (2018) model the progress of long-term recovery for individuals after a disaster. Others focus on the optimization of resource allocation to best serve the post-disaster needs of broader populations (Hu et al. 2016; Lubashevskiy, Kanno, and Furuta 2013). Foundational to both of these areas of inquiry is the study of recovery for individual infrastructure systems, such as power (Duffey 2019), transportation (Ganin et al. 2017), and gas pipelines (He and Nwafor 2017), as well as broader multi-infrastructure assessment (Bristow 2019; Zhao, Li, and Fang 2018).

One tool commonly used in North America for natural hazard analysis is Hazus, a software developed by the United States Federal Emergency Management Agency (FEMA). Hazus inputs include hazard categorization, geographic information, and infrastructure system data for a location of interest. This information is processed in Hazus and results are produced by applying data from empirical studies of previous hazards to the input information. Results include the probability of damage to different infrastructure components, as well as the likelihood of recovery for various systems after a specified amount of time (FEMA 2011). Dependencies within and between infrastructure systems are not explicitly modeled, so outputs are based on prior recovery trends from similar systems and expert judgement.

To address the recovery dynamics of multi-infrastructure systems by incorporating the interdependencies that connect them, Bristow and Hay present the Graph Model for Operational Resilience (GMOR) (Bristow and Hay 2017; Bristow 2019). GMOR models the components of infrastructure systems and the dependencies between them along with failure, repair time, and required repair resource information to track the recovery of systems over time.

3.3 Materials and Method

For the study presented here, physical entities for water, wastewater, electrical power, road networks are represented within a GMOR model by unique identifying parameters. Beyond these systems, others such as buildings, maintenance facilities, and supply networks may be added to the model in the future. The GMOR parameters include details like the type of entity (function, resource, event, or system), spatial information (if present), and any other entities within the model that a given component is dependent on (Bristow and Hay 2017). The parameters are combined into a city-scale model and used to generate five hundred randomized trials in a Monte Carlo fashion that allows estimates of the recovery timeline of the infrastructure to be produced.

Many of the parameters used in the GMOR model for this study are derived from Hazus information produced in a previous study on the vulnerability of infrastructure systems conducted by the federal government in the selected case study area. Inputs to Hazus for the previous study include geographical information about the District, as well as parameters for a magnitude 7.3 earthquake centred in the Strait of Georgia. Outputs from Hazus utilized for the study presented here include the probability of occurrence for varying levels of damage as well as repair and recovery parameters for the different infrastructure systems. Further details of this integration are included in the following sections.

The incorporation of dependencies is a key feature of GMOR that offers an improvement over modeling approaches that use individualized repair times for components without representing their reliance on other necessary systems and processes. GMOR only shows that an entity is functional once its upstream dependencies are functional as well.

Functionality of all systems in a given neighbourhood is represented by a single entity within the model that indicates that water, wastewater, power, and road networks within that neighbourhood have all been restored, and that the required dependencies for distribution and collection systems (see Section 3.3.2) are intact. The recovery time shown for this entity is simply equal to the highest calculated time for any one of the included systems and allows for quick evaluation of neighbourhood recovery as a whole, while also offering a view of the recovery times of individual systems.

For prioritizing the repairs done to the various infrastructure systems within the District, a random order is applied in the model. That is, there is no one neighbourhood that is consistently prioritized for repairs before the others in the model. Random ordering reflects the uncertainty involved in the location of damages that occur within a system and the possible location of repair resources at the time of a disaster. In addition, it provides insight beyond stakeholder assumptions into which ordering might produce the best results.

3.3.1 Study Area

The case study involves the District of North Vancouver (DNV), a municipality located in the southwest portion of British Columbia, Canada, across a marine inlet from the City of Vancouver. This largely suburban municipality is home to approximately 86,000 residents (Statistics Canada 2017), most of whom live in the southern portion bordering the City of North Vancouver. As seen in Figure 1, the northern part of the district primarily consists of sparsely populated, forested terrain.

The District is situated in an area that is subject to seismic hazard and is at risk of a large earthquake in the future. An earlier study conducted by the District in partnership with Natural Resources Canada (NRCan) and a number of other research partners examined the effects of an earthquake on local infrastructure systems. This study evaluated the likelihood and effects of known hazards in the region before completing a comprehensive assessment of a reference-case magnitude 7.3 shallow earthquake centred in the nearby Strait of Georgia. Hazard information for this earthquake was then processed with Hazus to determine the direct effects and

probabilities of failure of the various infrastructure systems of interest (DNV 2015; Journeay et al. 2015).

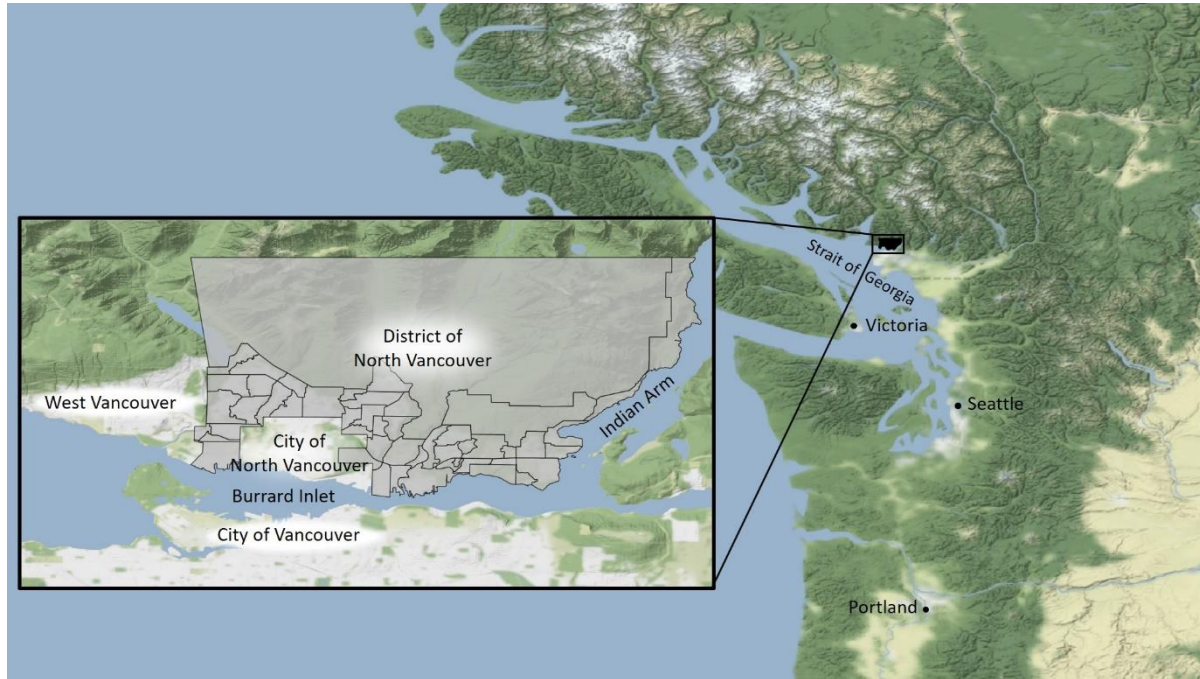


Figure 3-1: Map of Study Area and surrounding landmarks. Background map Stamen Design, under CC BY 3.0.

Hazus outputs include the estimated level of damage to various infrastructure components, and for some infrastructure systems, the probability of system recovery after a certain number of days. Instead of using this data directly, however, the goal of this study is to offer an estimate of recovery time for each component in the study area. To achieve this, the damage state reported by Hazus is coupled with repair times for the various systems. These repair times are gathered from federal partners involved in the earlier study as well as Hazus documentation (FEMA 2011), which is derived in part from a study of earthquake damage data developed by the Applied Technology Council (Applied Technology Council 1985), as well as expert judgement.

Separating damages and repair times provides flexibility to the process of modeling in GMOR. If improvements are made to recovery time estimates or local availability of resources,

these can be quickly incorporated into an updated GMOR model. In addition, this separation allows dependencies to be added to the GMOR model that are not represented within Hazus.

3.3.2 Included Infrastructure Systems

Infrastructure sectors included in this study are potable water distribution, wastewater collection, power distribution, and road and highway networks. Each of these systems is separated into zones based on neighbourhood boundaries within the District shown in Figure 3-1.

Water distribution and wastewater collection networks are connected by neighbourhood paths to central water supply and wastewater treatment facilities by a process shown in Figure 3-2. In this illustration, zone 14 contains the source or termination of an infrastructure system, such as a water distribution or wastewater treatment plant.

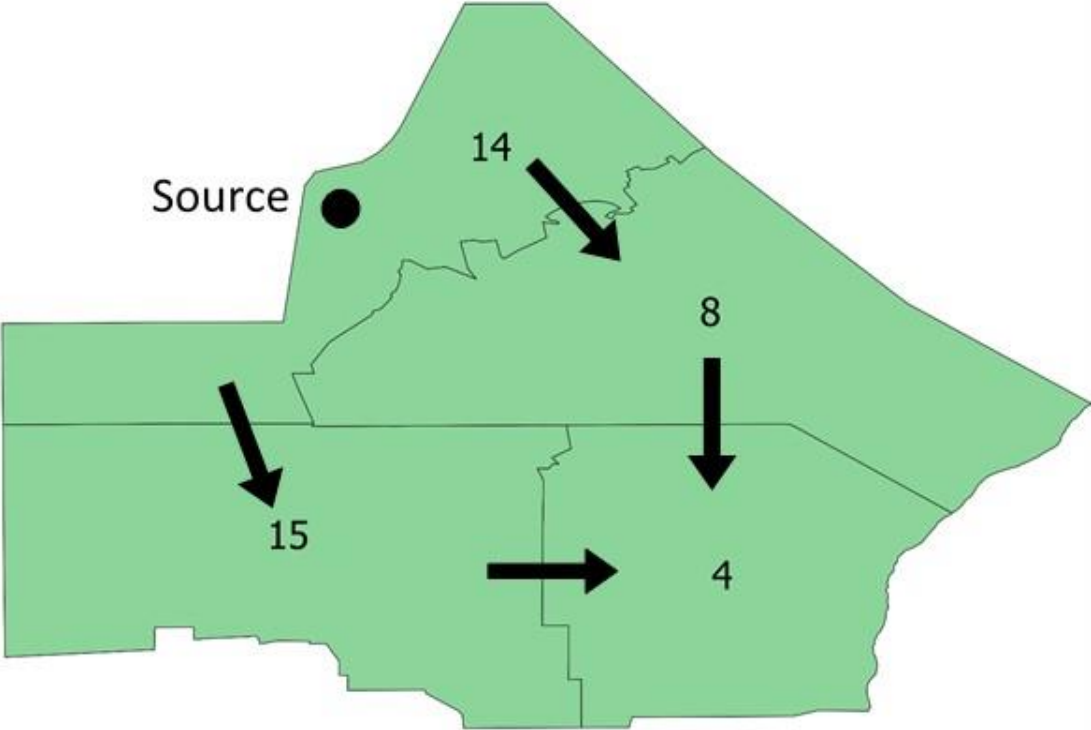


Figure 3-2: Path joins require a functional set of intermediate neighbourhoods to indicate recovery.

Power distribution and road systems are represented as isolated entities within neighbourhoods, with no reliance on systems in bordering neighbourhoods. Since power generation is largely located far outside the District, it is assumed that local network failures are the most significant cause of disruption at a neighbourhood scale and that lines entering the District remain in tact.

In the same way, damage to local roadways is assumed to present the most immediate disruption for residents. Redundancy in road systems and the capacity of repair crews to pass minor obstacles likely result in negligible delays to access repairs compared to the duration of the repairs themselves. In addition, modeling each individual road segment and its connection to other roads is computationally complex (though it is undertaken for a small part of the road network in Chapter 4), and the unknown location of repair crews relative to damaged components at the time of a disaster restricts modeling to a neighbourhood scale.

In this model, failures in the water distribution and wastewater collection networks are correlated to those established by the previous District study mentioned in Section 3.3. Power and road network failures are probabilistically determined based on federal partner data and Hazus outputs from the previous study as well.

3.3.3 System Failures and Recovery Time Parameters

Recovery time parameters and failure data for infrastructure systems are sourced from Hazus documentation and federal partner data and estimates. The application of this data to the current study is described below and further discussed in Appendix B.

3.3.3.1 Water Distribution and Wastewater Collection

For water distribution and wastewater collection systems, the times assumed for pipe repairs are shown in Table 3. These repair times are scaled by the number of breaks and leaks within a neighbourhood. The levels of damage and availability of repair crews are held constant, but recovery time varies based on the distribution indicated in the table.

There is a single water distribution facility in the district. In order for water distribution systems in other neighbourhoods to be functional, this facility must first be repaired. The system is largely gravity-fed but is supported by a transmission pumping system. Repair time for the pumping system is derived by correlating Hazus information with probabilities of damage and is calculated as a distribution with a mean of 2.83 days and a standard deviation of 1.34 days.

The district has one wastewater treatment facility located near the southern border of the District. In the same way that the water distribution system in each neighbourhood is joined to this facility by adjacent neighbourhoods, the wastewater collection network is connected in the same way. Each individual neighbourhood must be able to reach the facility by means of functioning neighbourhood wastewater treatment network entities in order to be restored to full function itself. Future studies may explicitly model individual pipe segments, redundancy provided by parallel systems, or critical sewer lines, but that complexity was not included here for the sake of computational efficiency and lack of data available.

3.3.3.2 Power Distribution

For the electrical power distribution system, the paths of power lines and locations of other key parts of the system are not available. Instead, damage and repair time is weighted by population at a neighbourhood level as described in Appendix B. Because path connections between neighbourhoods are unknown, the power distribution system in each neighbourhood is treated as independent for the purpose of repairs. As mentioned previously, it is assumed that power lines feeding into the district are functional, so the recovery modeled is for lines completely within the boundaries of the district. Low resolution provincial data indicates that multiple feeder lines enter the district, so the power system in the area already has redundant capacity. In addition, the power transmission and distribution system is established and maintained by a provincial organization. As a result, the district does not have much of an influence in making decisions about which lines are repaired first, and the model presented here only considers an approximate overall recovery timeline.

As indicated in Section 3.3.2, the power distribution network was not set to fail in all neighbourhoods in every trial. This is different than the water distribution and wastewater

collection systems, which are both set to fail in every neighbourhood in every trial. Instead, the probability of failure and recovery time for the power system in each neighbourhood is determined using federal partner data scaled by neighbourhood population. These probabilities range from a minimum of less than one percent to a maximum of one hundred percent, indicating that certain neighbourhoods do fail in each trial. Average repair time in individual neighbourhoods ranges from less than one day to almost 450 days. Due to a lack of available data, the standard deviation for each of these averages was fifty percent of the mean as follows for similar parameters in Hazus documentation.

Table 3: Summary of repair time parameters by repair task

Repair Task	Mean (Days)	Standard Deviation (Days)
Leak	0.313	0.156
Break	0.625	0.313
Water Distribution Facility	2.83	1.34
Power Distribution	Estimates from federal partner	
No damage	0	0
Roads Slight damage	0.9	0.05
(per km) Moderate damage	2.2	1.8
Extensive/complete damage	21	16

3.3.3.3 Road Networks

For road networks, Hazus repair times are given by the time required to repair a one-kilometre segment of road based on the level of damage they experience (Applied Technology Council 1985; FEMA 2011). These so-called “damage states” are grouped into four categories – no damage, slight damage, moderate damage, and extensive/complete damage.

The probability of occurrence of each damage state for road segments was produced in the previous District study. These probabilities are correlated with Hazus repair times and

weighted by the length of roadway to provide an overall probability for each damage state at a neighbourhood scale. The individual repair time parameters are included in Table 3 and further discussed in Appendix B. As indicated in Appendix B, the methodology used to establish failure probabilities and repair time parameters can result in extreme outliers in reported repair times. These outliers are further discussed in Section 3.4.

Road networks in this study are not joined by a path to a central hub or network, though Chapter 4 presents this capability for paths that connect pairs of origin and destination points. Instead, the road networks presented here utilize the damage state methodology discussed in detail in Chapter 2. This method offers flexibility for defining recovery parameters based on organizational data and integrates well with other damage estimation tools such as Hazus.

3.3.3.4 Sample GMOR Files

A sample of the files in the format that GMOR models use is given in Appendix C. These files show the format used to represent the varying types of infrastructure systems modeled in this study, including the structure of path dependencies for water and wastewater shown in Figure 3-2, isolated systems like the power network discussed in Section 3.3.3.2, and the multiple damage state methodology for road networks mentioned in Section 3.3.3.3.

3.3.4 Interdependent Systems and Restoration Resources

Dependencies between systems are limited in this study due to their functional separation within the District. The exception to this is water distribution and wastewater treatment facilities, which depend on electrical power within their respective neighbourhoods. This dependency is discussed further in Sections 3.4.1 and 3.4.2. In addition, it is understood that road access is generally required to perform repairs on many systems. As mentioned in Section 3.3.2, however, the time required to access damaged components is likely less of a concern than the damage of the components themselves.

Information from the district and federal partners indicate that repair crews are specialized in the work that they perform, so cross-sector restoration resource sharing is unlikely. In different municipalities or studies with different levels of resolution, there may be conflicts in

restoration timing due to resource sharing across sectors such as equipment or labour that would need to be included in the model.

3.4 Results and Discussion

Results are presented here for the different infrastructure systems explored in the case study. Separating the results into the varying domains of interest gives insight into which systems might be the most exposed in an earthquake and may benefit from additional preparation and protection. The initial failures for the different sectors of interest are shown in Figure 3-3.

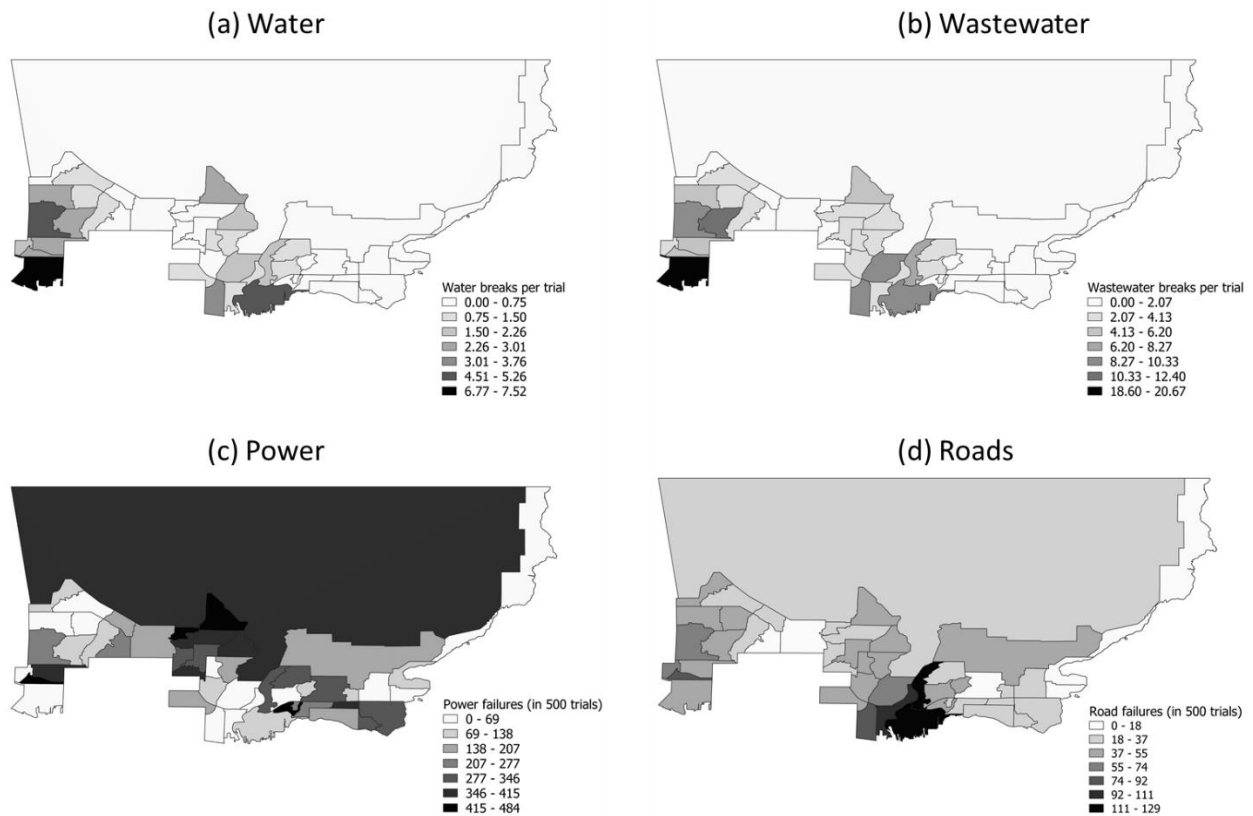


Figure 3-3: Failure characterization by neighbourhood for (a) Water distribution; (b) Wastewater collection; (c) Electrical power distribution; and (d) Road and highway networks. Water and wastewater are categorized by number of breaks per neighbourhood, while power and road networks are categorized by total number of failures indicated out of 500 trials.

3.4.1 Water Distribution

The variation in the recovery times of water distribution is shown in Figure 3-4. The percentage on the vertical axis the figure indicates the number of neighbourhoods (out of 49) that are recovered at the time indicated on the horizontal axis. The "Average" line plots the average time taken (in all trials) for one neighbourhood to recover, then two neighbourhoods, and so on, regardless of the location or population of the neighbourhood. The mean repair time for the neighbourhood across all trials is 54.8 days with a standard deviation of 14.5 days. As shown in Figure 3-4, the shortest repair time observed for repair of all neighbourhoods in the District is 56.8 days (best case), while the longest repair time is 87.9 days (worst case).

Central to the variation in recovery time of neighbourhoods is the path dependencies mentioned in Section 3.3.2 and their interaction with the ordering of repair of the neighbourhoods. This effect is illustrated in Figure 3-4, where large jumps in the number of recovered neighbourhoods in the best and worst case demonstrate that the repair of certain neighbourhoods leads to the recovery of many others that are dependent on it. This is especially apparent in the worst trial scenario, where over two months pass before a single neighbourhood is recovered. Identifying which neighbourhoods were recovered at the time of one of these jumps lends insight into the neighbourhoods that may be bottlenecks for recovery and should be prioritized to expedite overall recovery. Correlating these neighbourhoods with their populations could provide further understanding of the effects of prioritizing low-population, highly connected neighbourhoods over those that have high populations but are located far from the distribution source.

Note that Figure 3-4 shows recovery only for the pipelines within the water distribution system and does not include the dependence of some neighbourhoods on electrical power distribution. This decision was made to better show trends of recovery in the District and eliminate extreme outliers from the data set. Further, it is assumed that emergency provisions (such as backup power) can be made for water systems to supply neighbourhoods as necessary. Widespread power recovery may take longer, but functionality for critical systems like water distribution are likely to be restored sooner.

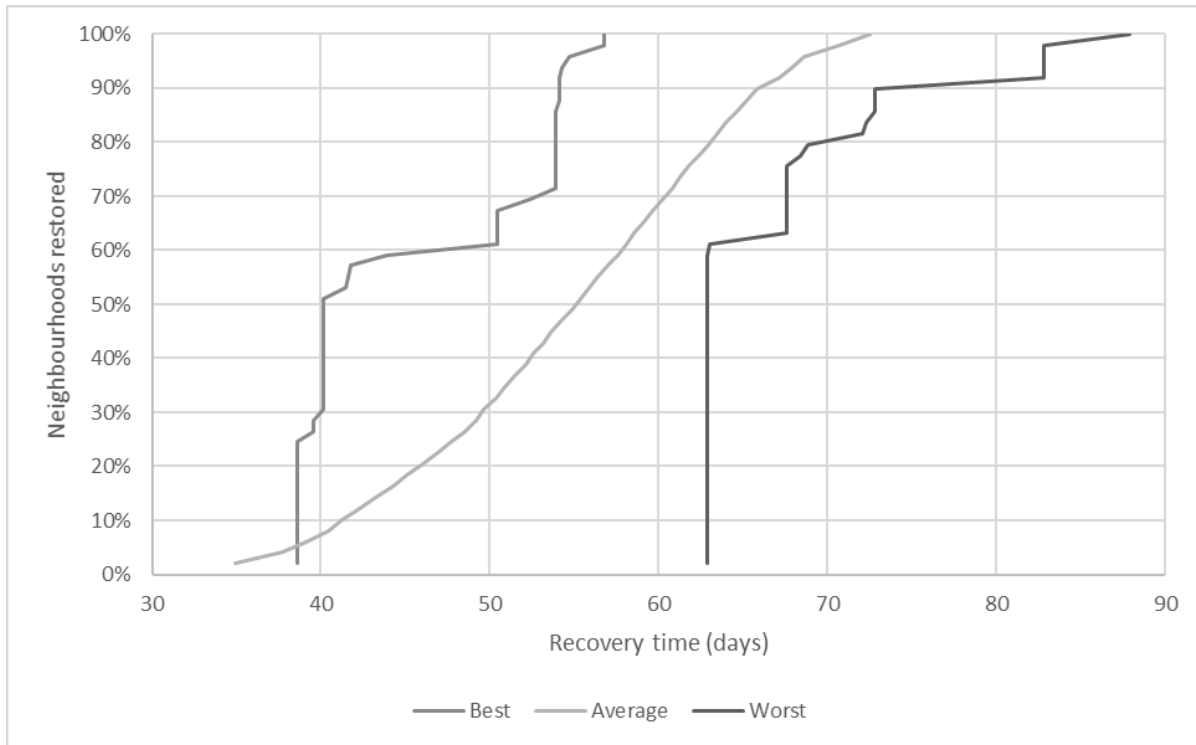


Figure 3-4: Best, average, and worst-case scenario recovery times for the water distribution system in the District. Note that best and worst correspond to fastest and slowest overall recovery of all neighbourhoods.

3.4.2 Wastewater Collection

The average repair time of the wastewater collection network for any given neighbourhood in any trial is 42.8 days, with a standard deviation of 25.3 days. For the whole district, the average recovery time for the wastewater collection network is 87.2 days (Figure 3-5), with a standard deviation of 5.4 days. The lower variability in overall recovery time illustrates the effect that ordering and path dependencies have on neighbourhood recovery. While individual neighbourhood recovery times can vary drastically due to the order in which they are addressed, the overall recovery time remains relatively more consistent as repairs in well-connected neighbourhoods trigger recovery for many dependent neighbourhoods at once.

The maximum recovery time calculated is 103 days, and the minimum is 72 days. The variability in the wastewater collection network is smaller to that of the water distribution

system, indicating lower individual variability in recovery times at a neighbourhood level. This is confirmed by the source data, where the average deviation in wastewater collection network recovery time is lower than the deviation in the water distribution network.

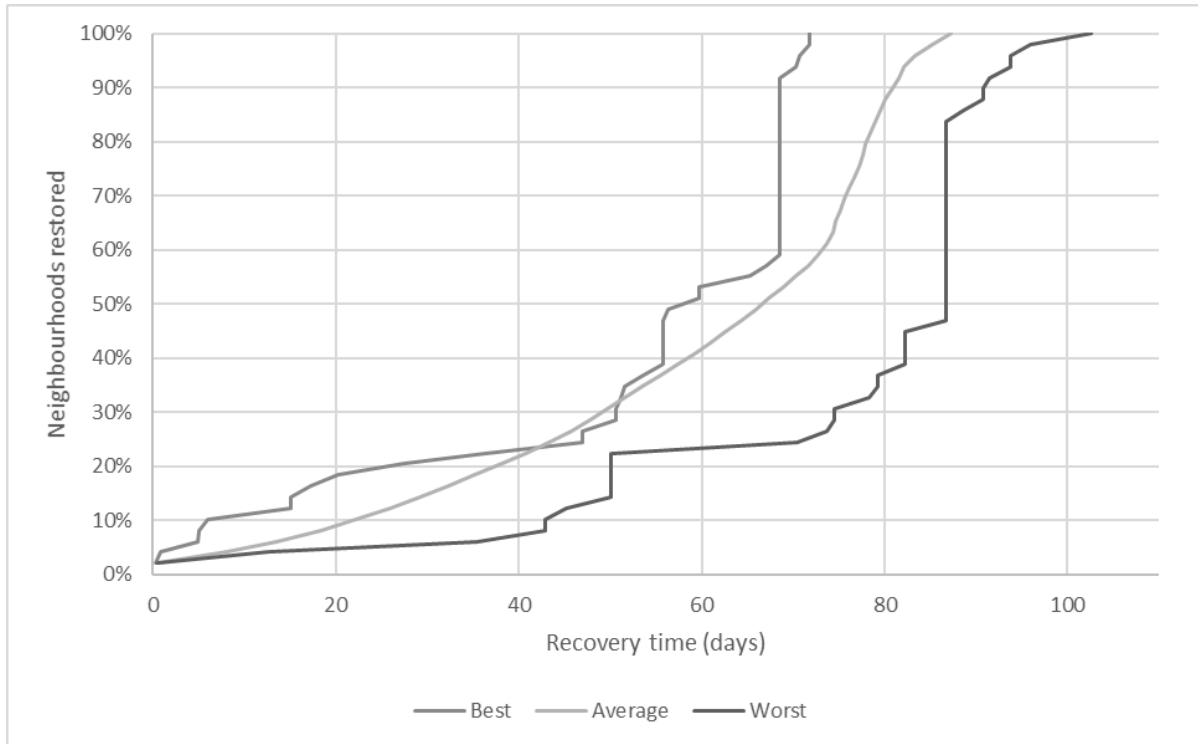


Figure 3-5: Best, average, and worst-case scenario recovery times for the wastewater collection network in the District. Note that best and worst correspond to fastest and slowest overall recovery of all neighbourhoods.

As is the case for the water distribution system, there is a dependence on power for the wastewater collection network in one of the District’s neighbourhood. This dependency was assumed negligible for the purposes of these results for the reason indicated in Section 3.4.1 (i.e., the expected use of backup power).

3.4.3 Electric Power Distribution

Average recovery time of the electric power distribution system for any neighbourhood in a trial was found to be just over 61 days with a standard deviation of over 123 days. Note that these values include trials and scenarios in which the power network did not fail. As such, many of the

values considered in the average and standard deviation calculations are zero, which skews the results. If these scenarios are ignored, average recovery time jumps to almost 158 days with a standard deviation of 155 days. This large increase in required repair time indicates that the electric power distribution system is very sensitive to disruption in that failures have a substantial impact on the resources and time required to return the system to an operational state.

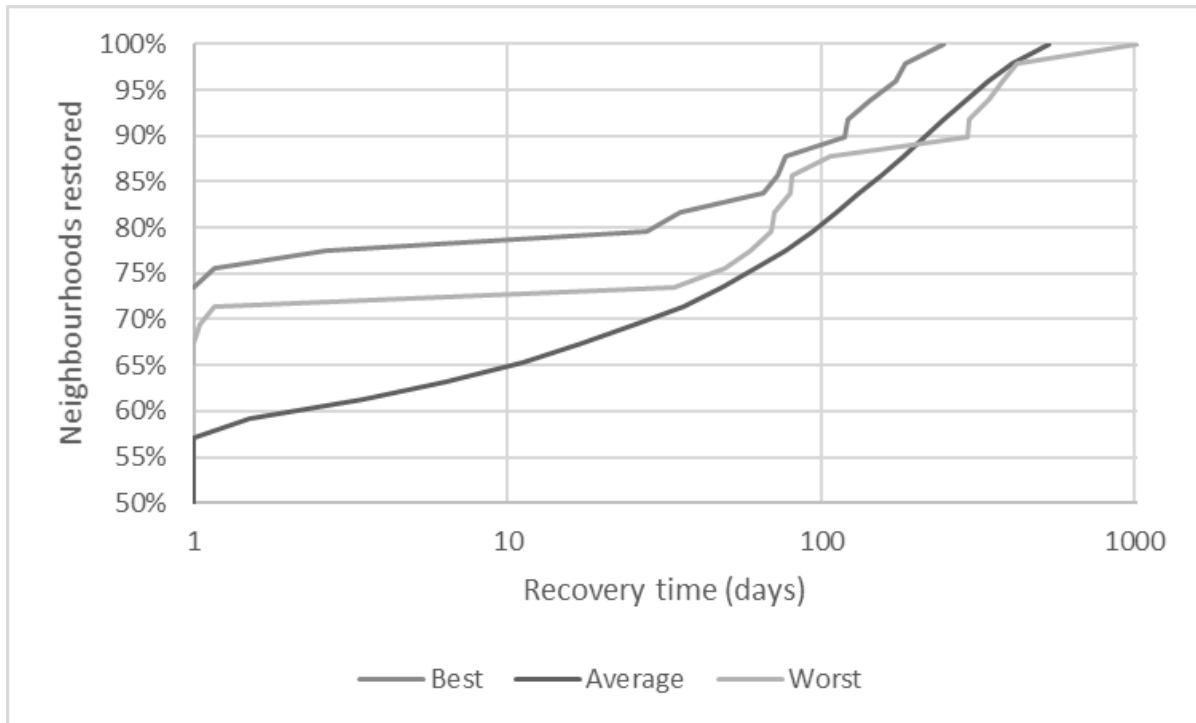


Figure 3-6: Best, average, and worst-case scenario recovery times for the electric power distribution network in the District. Note the logarithmic scale on the horizontal axis and that best and worst correspond to fastest and slowest overall recovery of all neighbourhoods. As such, even though the worst-case scenario progresses more quickly than average for most of the District's recovery, delays in later neighbourhood recovery significantly increase the overall recovery time.

The greatest number of neighbourhood failures experienced in a single trial is 26, and the least is twelve. That is, out of the 49 neighbourhoods in the District, at least 12 and at most 26 are predicted to fail in any trial. While it may be useful to see how many neighbourhoods fail in each trial to observe areas that are particularly vulnerable, the number of failures is not an

accurate indicator of recovery time in the District given the variability in individual neighbourhood recovery time.

The overall average recovery time for the District for the power system is just over 531 days, with a minimum of 245 days, a maximum of 1,013 days, and a standard deviation of 140 days, as shown in Figure 3-6. There is a high degree of variability in the repair time of the power network, largely because it is tied to the population in each neighbourhood. While population serves as a valuable proxy for the scale of many infrastructure systems, incorporating the actual layout of the power system would increase the accuracy of future models.

3.4.4 Road Networks

As mentioned in Section 3.3.3.3 and Appendix B, the methodology used to establish road failure probabilities can lead to extreme outliers in the dataset. A histogram of repair times for the whole road network in the District including these outliers is shown in Figure 3-7. The mean repair time for this data set is 451 days, with a standard deviation of 519 days. This includes eight scenarios in which no failures were indicated, so the minimum repair time for the road network in the District is zero days, while the maximum is almost 4,700 days.

As indicated in Figure 3-7, repair values are largely concentrated in the lower end of the range shown. The outliers are left in this data set because it is important to recognize the effect that a catastrophic disaster could have on the District. Planning activities, however, should largely focus on the more realistic scenarios represented by the centre of the box plot shown in Figure 3-10.

Figure 3-8 shows the road network recovery over time in the District. Note the logarithmic scale on the horizontal axis and the large discrepancy in average versus worst-case scenario recovery. Shortest recovery time is not shown in Figure 3-8 due to the number of trials which indicated a repair time of zero days.

3.4.5 Overall Recovery

Note that the fastest overall District recovery time for the scenarios tested is longer than any of the fastest recovery times for individual systems. This is the result of the low likelihood of an ideal recovery scenario for one sector occurring in the same trial as the best-case scenario for all systems. However, combining ordering and resource parameters from the best-case scenarios for all trials can help inform decision-making that leads to improved repair time for the whole District.

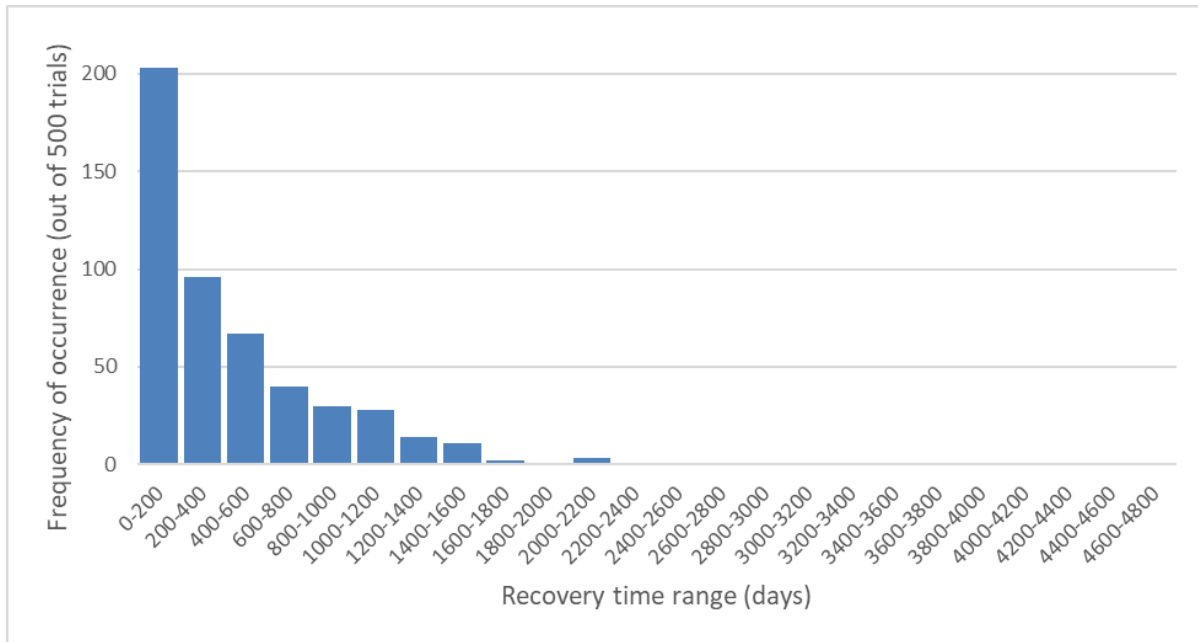


Figure 3-7: Distribution of road network repair times for 500 trial scenarios.

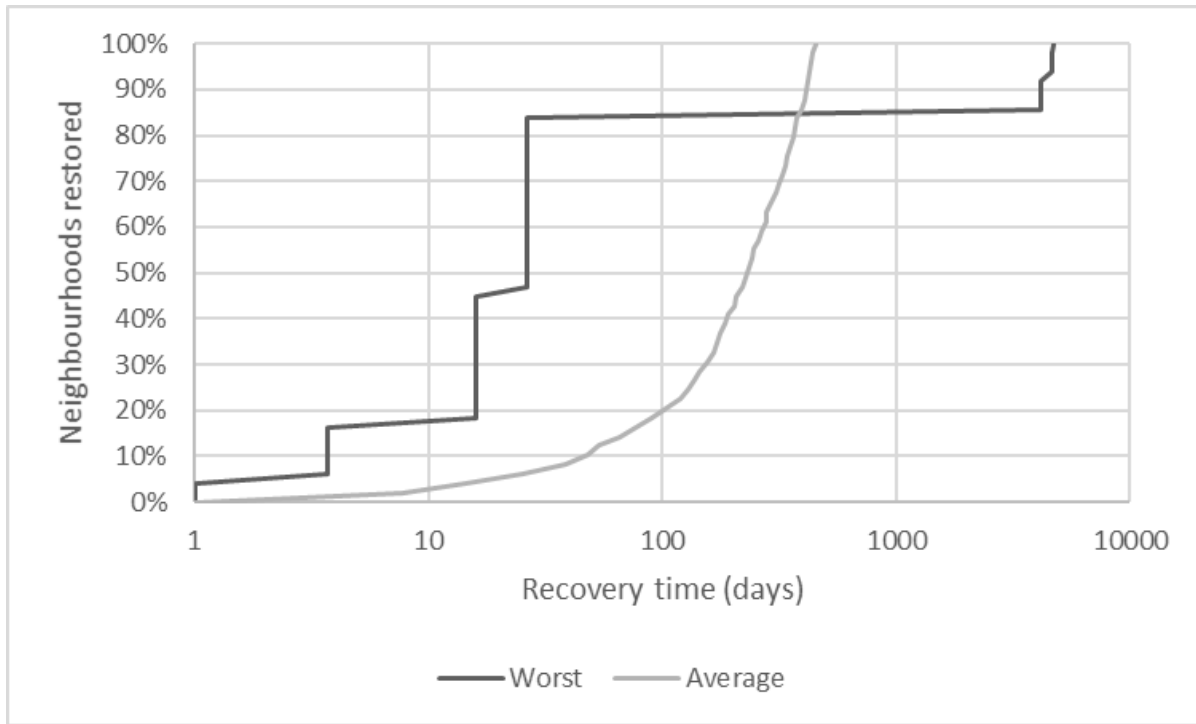


Figure 3-8: Average and worst-case scenario recovery time for neighbourhood road networks in the District. Note the logarithmic scale on the horizontal axis. As is also seen in Figure 3-6, the worst-case scenario for road network recovery starts off much faster than average, but significant delays near the end of the restoration period lead to a much longer overall repair time than average.

Overall recovery in the district averages 702 days, with a standard deviation of 404 days. The shortest recovery time indicated is 252 days, while the largest is 4,685 days. In general, the repair time of either the road network or power distribution network governs the recovery in the District as a whole.

Note that the scale of the horizontal axis of Figure 3-9 is logarithmic, indicating substantial horizontal jumps that are representative of large individual repair times for specific entities. In general, these jumps are the result of a combination of a rarely experienced high damage state and a repair time in the top range of a normal distribution. These extreme scenarios should certainly be considered in planning for disasters, but are by no means representative of the level of damage and repair times that would likely be experienced in the District.

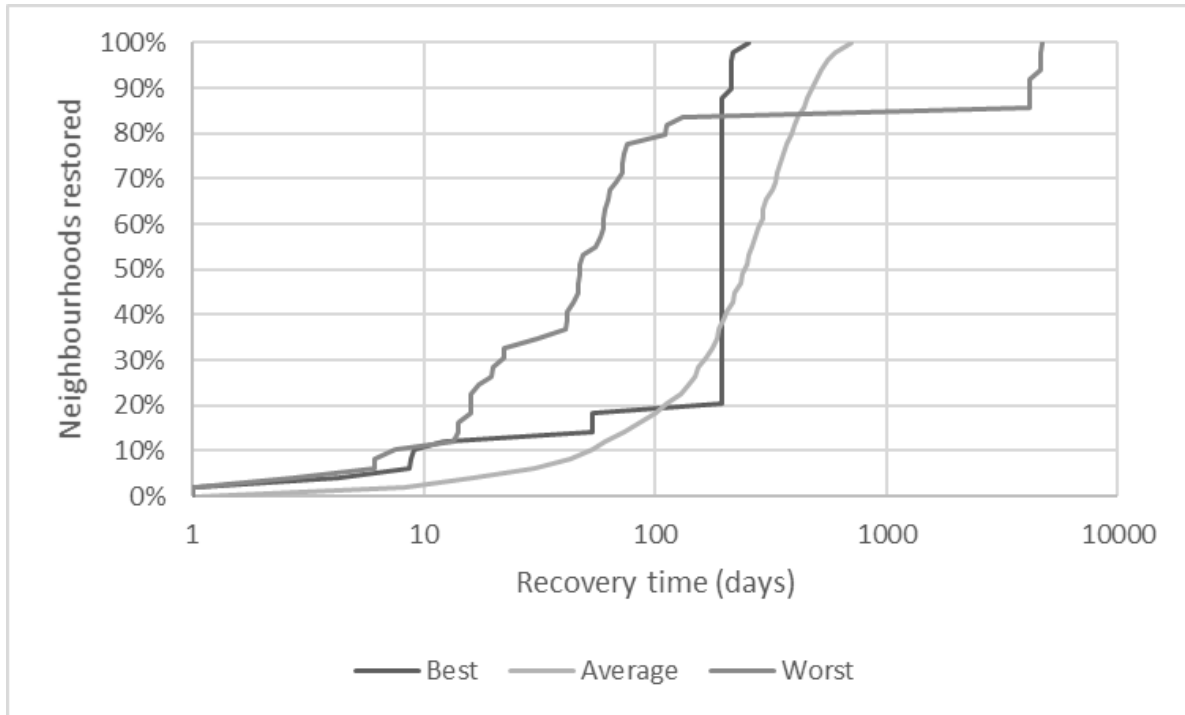


Figure 3-9: Overall recovery time of all systems within the District. Note the logarithmic scale on the horizontal axis, and the categorization of best and worst repair times based on the fastest and slowest repair times indicated, respectively.

The central portions of the box plots shown in Figure 3-10 represent a more realistic view of the repair times that planners, emergency service personnel, and residents should prepare for following a disaster. The “End Users” plot represents the overall recovery time for the neighbourhoods within the district.

3.4.6 Discussion of Results

These results can offer insights to emergency management organizations and planners by estimating the duration of emergency or supplementary services needed after a disaster. By providing results at a neighbourhood level, infrastructure managers can prioritize which areas will need the most attention for repairs and arrange for adequate resources in those locations. Residents can also be informed within their neighbourhoods about how they can best prepare themselves for a disaster, especially by understanding which lifelines might be most at risk in their area and how they can function if those lifelines are out of service.

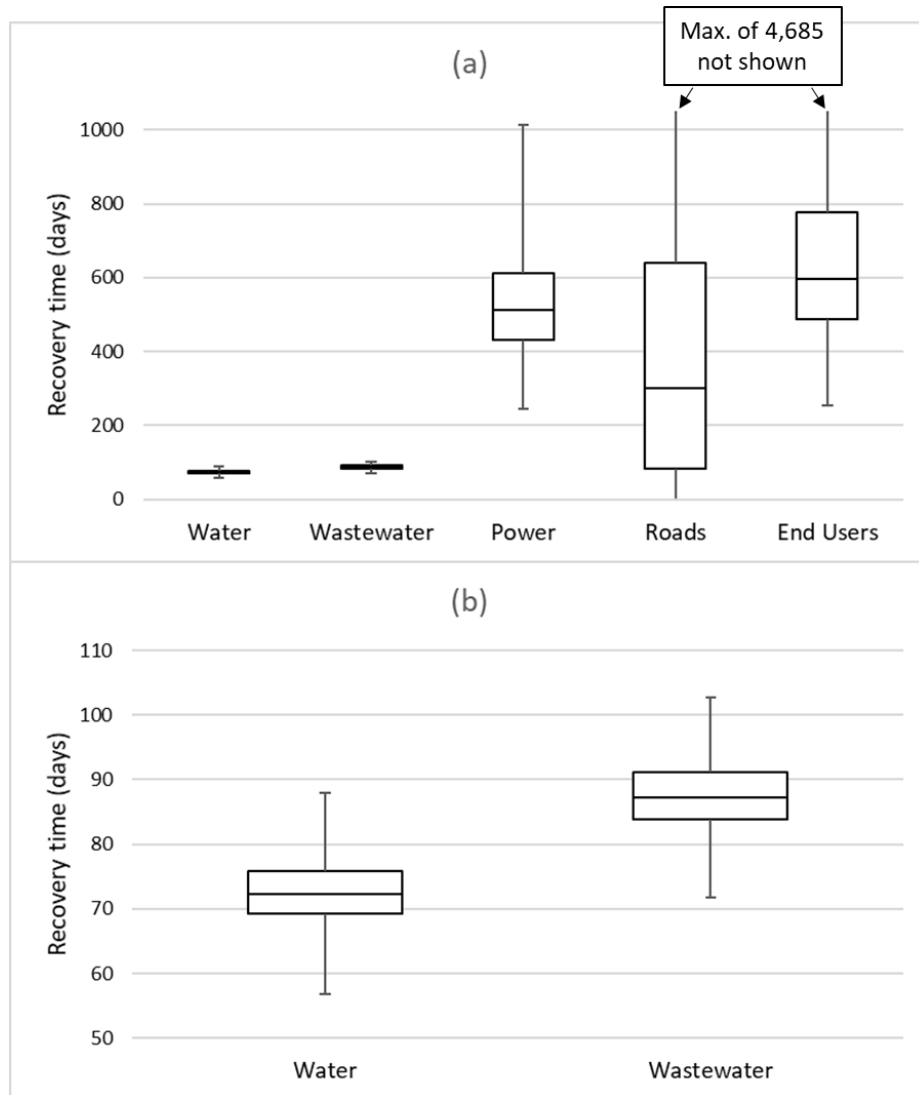


Figure 3-10: Box plots for (a) all studied infrastructure sectors in the district; and (b) water and wastewater systems. Note the different scales on the vertical axis of (a) and (b). The bottom and top tails of the plot represent the lowest and highest quartiles of data, respectively, while the box represents the second and third quartiles with the median indicated.

Associating these results with economic data can also help quantify losses in the District in the aftermath of a disaster. If managers and planners have a better understanding of how a disaster will impact their systems and residents, they may be driven to invest in disaster risk reduction strategies, which will improve outcomes for the district as a whole.

3.5 Conclusion

This study presents a city-scale data-driven model of multi-infrastructure recovery in a suburban municipality. Key findings indicate that repair times for electrical power and road networks are highly variable and influential in the overall recovery of neighbourhoods within the District. Other infrastructure systems are individually variable in their repair times, but do not affect overall recovery to the same extent that power and road networks do. Water and wastewater systems are expected to recover most quickly for the studied seismic event. It is important to note that these repair times represent full recovery of the systems studied rather than the time at which society can adequately function and prevent further losses after a disaster. Partial functionality to some sectors may provide an opportunity to expedite repairs in others. Therefore, an awareness of the ways in which neighbourhoods can continue to function while disaster recovery occurs is essential to improving outcomes for residents after a disaster.

Lessons learned from this study can inform the process of developing models for future work and improve the understanding of recovery in urban and suburban areas. Recognition of the influence of different infrastructure sectors on recovery will guide data collection for future studies in order to reduce uncertainty throughout the modeling process.

There are many opportunities to advance this form of data-driven modeling. The effect of altering the ordering of repair for different infrastructure sectors is substantial and can be challenging to include due to the data required about the underlying infrastructure network. Obtaining this data requires close collaboration with infrastructure operators. Further, while this study does not incorporate other functions that may exist within neighbourhoods, such as fuel stations or important buildings, future studies can include these entities to inform priorities for repair. For example, if a certain neighbourhood contains a hospital and emergency shelter, it may be more critical to send repair resources to that neighbourhood before another neighbourhood in an industrial area, or an area with low population. As more data becomes available and more needs are identified, modeling should be continually improved to best protect infrastructure systems and the residents and communities that they support.

4 Critical Road Network Recovery

4.1 Introduction

The District of North Vancouver (DNV) is located in southwestern British Columbia, just north of the City of Vancouver. This area is at risk of a large seismic event in the future and as a result has been subject to an extensive study detailing the effects that a magnitude 7.3 earthquake would have on the District's residents, buildings, and critical infrastructure lifelines. These lifelines are discussed in aggregate in Chapter 3. The work presented in this chapter provides additional assessment of the road network in a critical area of the District and offers a comparison of two resource prioritization methodologies

Given the earthquake hazard in the District, determining areas of damage that would critically impact transportation routes is essential to understand how resource distribution may be affected after a disaster. Based on results from the previous study, a map of road damage within the different neighbourhoods in the District was established and can be seen in Figure 4-1.

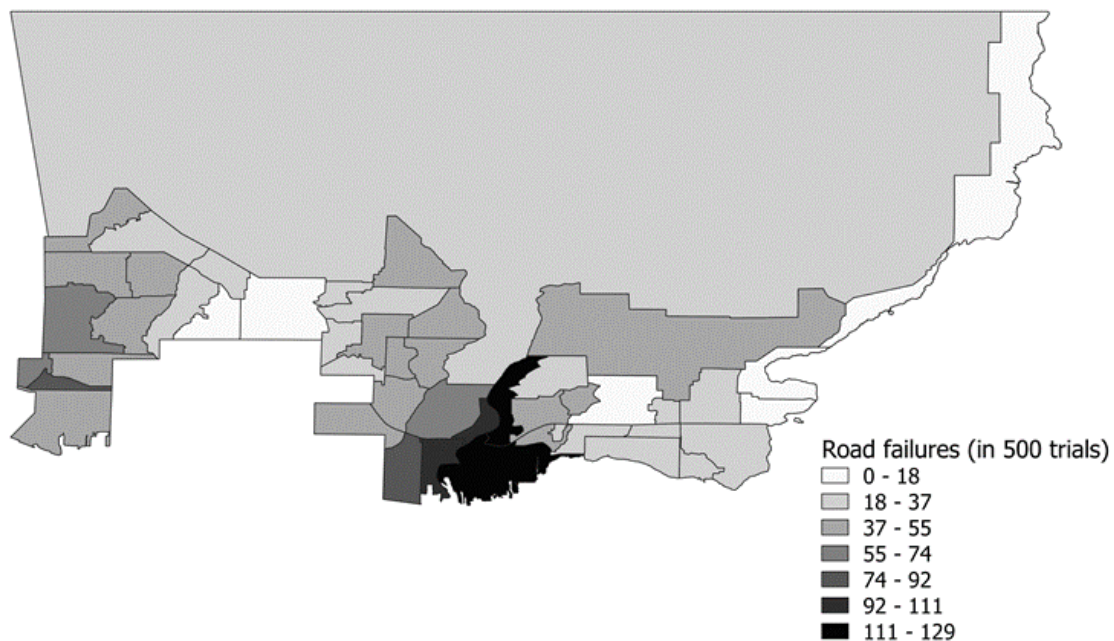


Figure 4-1: Number of road segments with damage in each neighbourhood in the District of North Vancouver based on 500 trial scenarios

The darkest sections of the map indicate the areas that are most likely to experience road failure in a disaster. This area happens to be in a critical location given its importance in connecting the west and east parts of the District, as well as connecting the east part to the City of Vancouver to the south.

The east and west parts of the District are separated by Lynn Canyon and the Seymour River, as shown in Figure 4-2, isolating a central part of the District that connects the two sides of the District. Three roadway bridges cross Lynn Canyon to connect the west and central sections, and another two bridges connect the centre and the east. Another bridge spans the Burrard Inlet to connect the central part of the district to the City of Vancouver to the south.

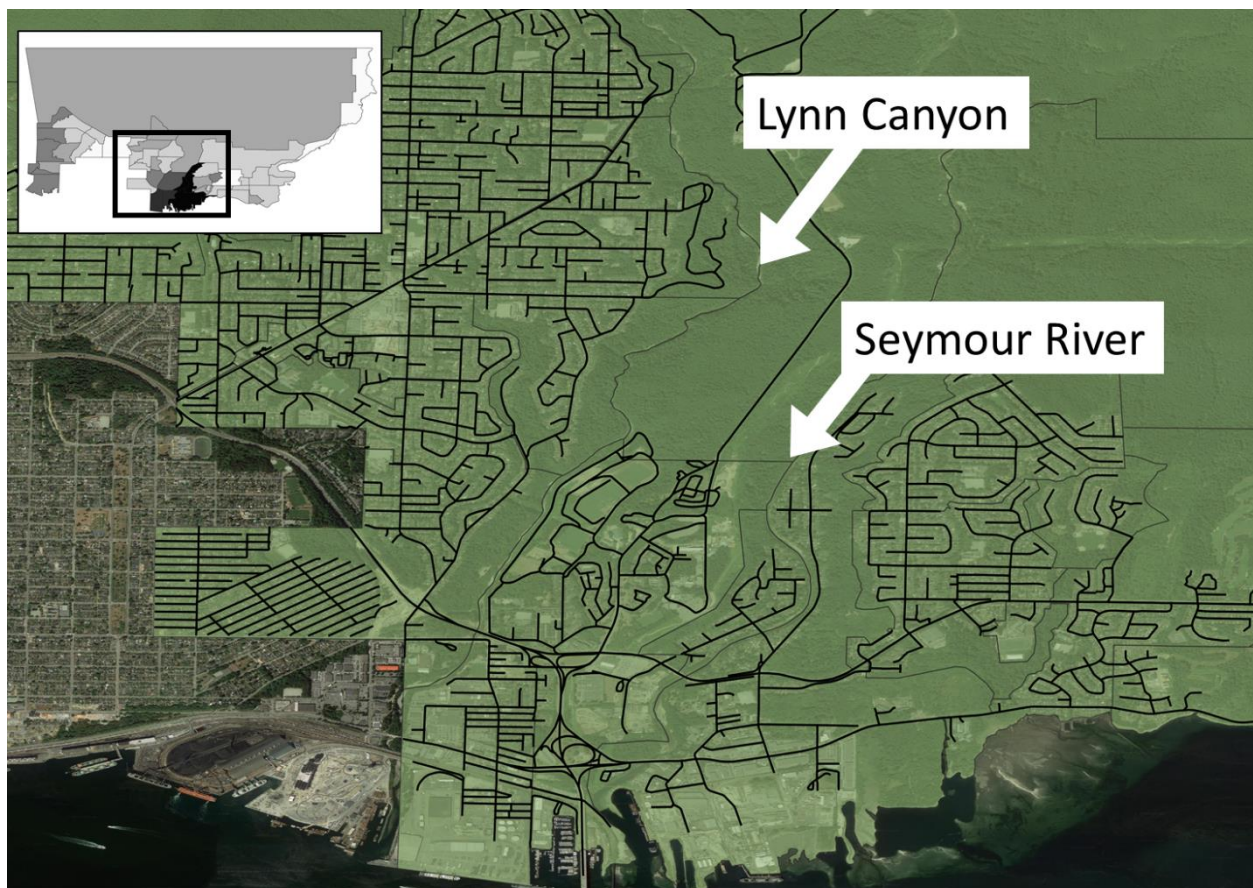


Figure 4-2: Overview of the area around Lynn Creek/Canyon and the Seymour River. Top left map shows enlarged area in the context of the whole District. The Burrard Inlet is directly south of the area shown. An overview of the surrounding area can be found in Figure 3-1.

While the west and central parts of the District are well-connected to West Vancouver, the City of Vancouver, and the west coast of the mainland of British Columbia, the east part of the district is bounded to the north by forested terrain and to the east by Indian arm. No other roads to external locations are available within the eastern part of the District. There is no airport serving the District, but commercial shipping docks are available along the Burrard Inlet. Transportation by rail was not considered in the study in Chapter 3 and is therefore not included as an available transportation option in this chapter.

This chapter focuses specifically on the recovery time of roadway transportation routes within the central part of the District based on the level of damage considered in previous studies and estimated repair time data gathered from previous disasters. The recovery is based on the functionality of three origin points in the west and south of the study area, and two destination points in the east. These points represent critical locations that, once functional, can be assumed to provide reliable transportation between the other parts of the district. Roadway paths are established between the different sets of origin and destination points in a process described in Section 4.3. A key goal of this chapter is to identify improvements in connection time by altering the priority of repairs for the various road segments in the study area.

In the neighbourhoods containing the study area presented here, the population consists of just over seven thousand people. Additionally, more than twenty thousand residents live in the eastern part of the District and are dependent on the road networks identified in this chapter as their only overland connection to the rest of the District. The study area consists of mostly residential communities, but some industrial areas operate in the south, with a railroad running along the border near the Burrard Inlet. Given the lack of other transportation options, a functional road network is essential to provide consistent access to goods and services coming from other areas within the District and outside of it. Access to medical services is also a concern, as the nearest hospital is located near the western part of the District.

In order to test the feasibility of the methodology used in this study, roads in the central area of the District were selected for a full assessment in this study. This area is shown in Figure 4-3 and includes the three east-west bridges that span Lynn Canyon, the north-south bridge that crosses the Burrard Inlet, and two bridges that cross the Seymour River. The roads are in the

area that is subject to the most extensive levels of damage identified in previous studies (shown in Figure 4-1) and are considered crucial for connecting the eastern and western parts of the District.

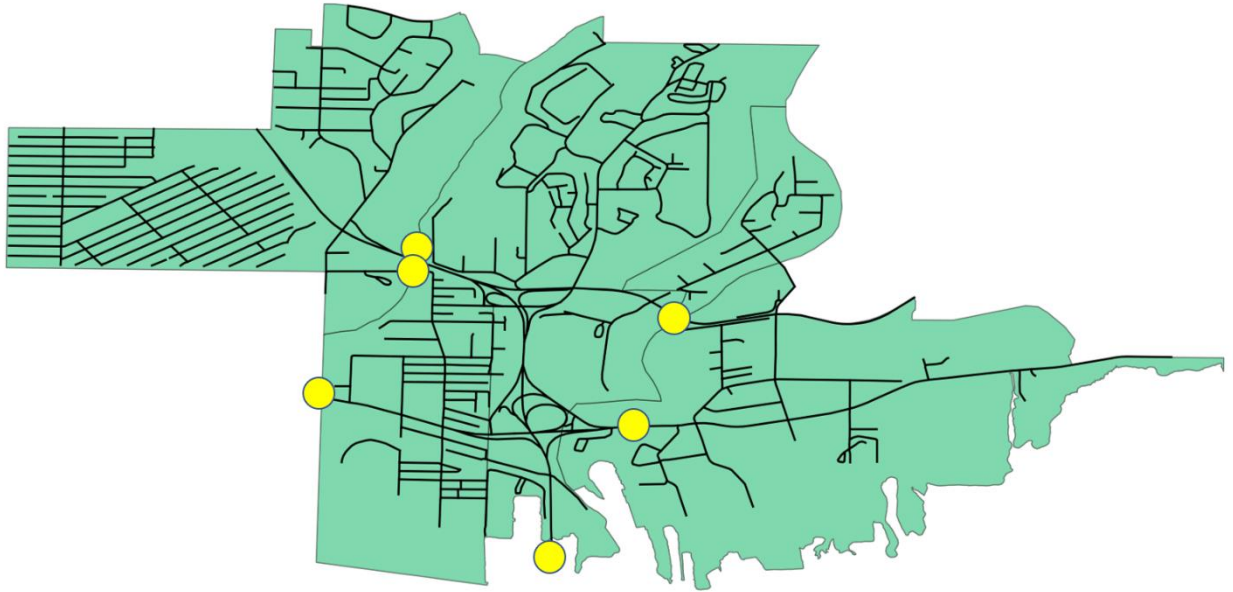


Figure 4-3: Neighbourhoods in study area with bridges highlighted.

4.2 Background

Most studies related to damage, repair, and restoration of roads can be grouped into a few main categories: planning repairs for standard road maintenance activities; measuring the level of damage and planning access and repairs of road networks due to natural or other disasters; performance characteristics of novel road repair techniques and materials; and optimizing road repair activities.

Janani et al. (2019), Donev and Hoffman (2018), and Lempert et al. (2016) address resource constraints, optimization of maintenance schedules, prioritizing repairs, and work zone planning for pavement repairs. These studies focus primarily on standard road repair activities and do not address emergency repairs or extensive levels of damage to road networks. Other studies consider full-depth reclamation of roads (Bocci et al. 2014) and are chiefly interested in

the performance characteristics of the rehabilitated roads. With respect to road damage after disaster, Anbazhagan, Srinivas, and Chandran (2012), Robinson (2018), and Gao and Sun (2012) have studied methodologies for categorizing damage as well as the impacts of failed roads on communities, while others provide an assessment of material performance after emergency repairs are conducted (Hawa et al. 2013; Howard et al. 2014).

Very few of these studies explicitly mention the repair times of roads. One exception is Li and Teo (2018), which indicates a standardized value of 0.5 kilometres of repairs per hour, but does not differentiate based on the level of damage that the road experiences.

One reference that does include information related to road repair time is Hazus documentation, which is produced by the United States Federal Emergency Management Agency (FEMA 2011)². The Hazus technical manual indicates mean repair time and standard deviation per kilometre of road based on the level of damage experienced. Background data used in Hazus documentation is provided by the Applied Technology Council's ATC-13 document, which is based on results from surveys of experts involved in repairs conducted after a number of earthquakes in California (Applied Technology Council 1985). While Hazus results are useful in providing overall repair times for road networks, the work presented here seeks to detail more fully how prioritizing the repairs of specific road segments affects the overall recovery time of the network.

To process the information gathered from Hazus related to the road repairs, Bristow and Hay's Graph Model for Operational Resilience (GMOR) is utilized (Bristow and Hay 2017; Bristow 2019). The capabilities provided by GMOR allow for the generation of paths to connect points of interest in the road network, prioritization of repairs, variation of repair times based on level of damage, and consideration of dependencies for the functionality of each entity within the model. Resource constraints can also be added to the model if desired, but are not included for the purposes of this study. Repair times indicated in ATC-13 and subsequently included in Hazus documentation clarify that restoration "follow[s] normal nonemergency construction schedules" (Applied Technology Council 1985). Since the size and capabilities of repair crews

² For further information about Hazus, see Section 3.2

in the original survey data is aggregated from a variety of sources, the repair times indicated in Hazus documentation are assumed to be accurate for use in the GMOR model as well.

4.3 Methodology

4.3.1 Network Creation

Road data from a GIS model of the District is shown in Figure 4-4a along with the selected origin and destination points mentioned in Section 4.1. Note that the locations of the origin and destination points are similar to the locations of the bridges shown in Figure 4-3.

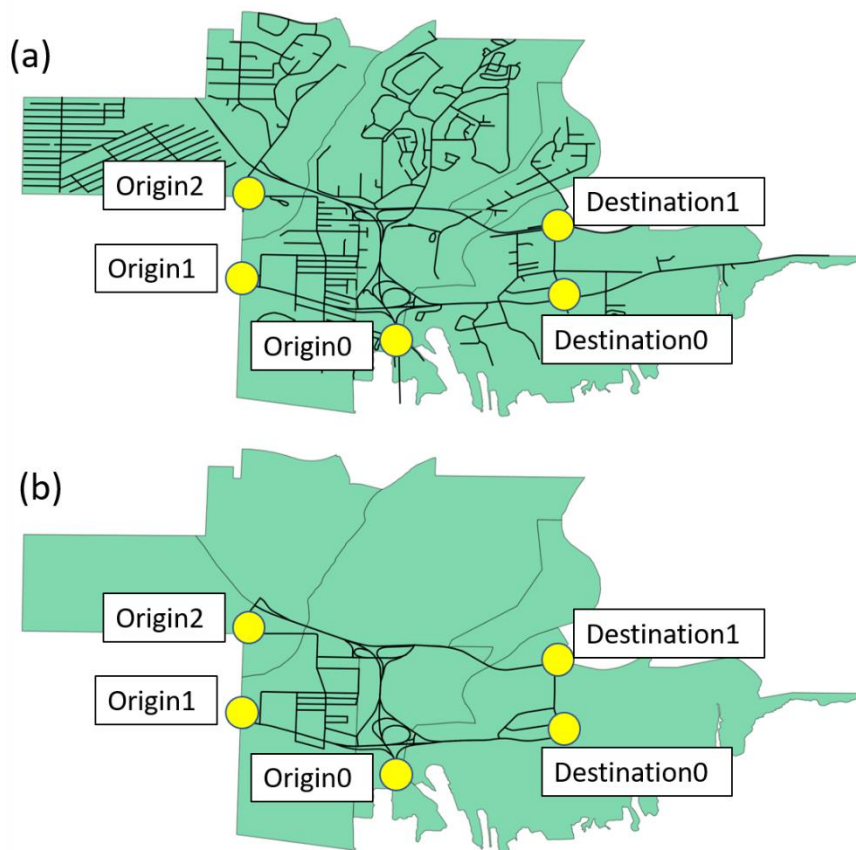


Figure 4-4: Selected origin and destination points with: (a) Full road network in study area neighbourhoods; (b) Simplified road network with most dead-end and extraneous roads removed.

From this data, dead-end roads and a number of extraneous road segments are removed to produce the model shown in Figure 4-4b. Each origin point, destination point, and road segment is associated with a unique identifying number which is then used to create a node in a graph model. These nodes are joined by edges that represent the connections between the roads in the study area. A simple example of a graph with nodes and edges is shown in Figure 4-5. In the graph, circles are the nodes that represent roads and points of interest, and lines (edges) represent the intersections that connect the roads.

Using computational tools for processing graph models, a set of shortest paths between each origin and destination points is produced. These paths are determined by the number of nodes (road segments) between the origin and destination, rather than by the length of the road representing each node. As such, the paths represented may not be the shortest by distance, but this difference is assumed to be negligible and negated by the number of paths identified between each origin and destination point.

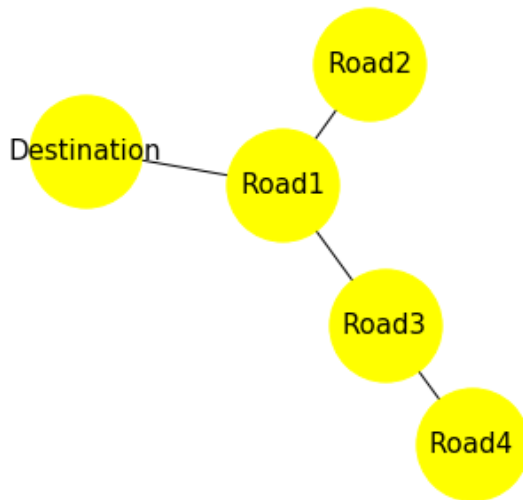


Figure 4-5: Example graph model showing nodes (circles) and edges (lines).

One issue encountered while working with the paths in the model is related to a lack of differentiation between one- and two-way roads. Data from the district does not indicate if a road is limited to one-way travel or is accessible in two directions. As such, situations arise in

which the shortest identified path includes a separated road that cannot be travelled as indicated, like the example path shown in Figure 4-6a. Road 2 can be accessed from Road 1, and Road 3 can be accessed from Road 2, but traveling from Road 1 to Road 2 to Road 3 directly is not possible.

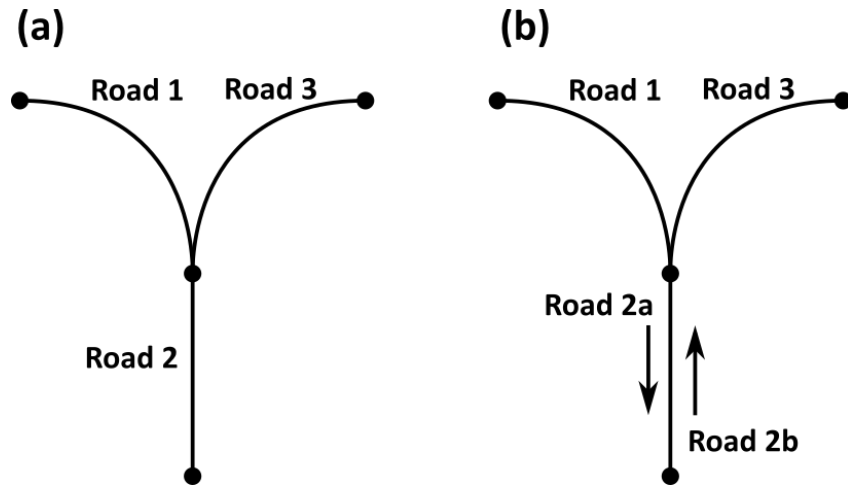


Figure 4-6: Additional road creation for roads with travel direction constraints.

To remedy this issue, new road entities are created and constraints added which indicate that vehicles can travel in only a single direction. This is shown in Figure 4-6b, where Road 1 can access Road 2a, and Road 2a can access Road 3, but there is no connection between Road 2a and Road 2b. Currently the process of creating separate road entities is done manually. Automating the creation of single direction road entities would improve efficiency in the future, especially for large models. New sections of road are assigned unique object identifiers to differentiate them in the GIS file and GMOR model.

After the creation of new road segments, the shortest path process is repeated and routes are manually checked for feasibility. The number of paths identified for each origin and destination is shown in Table 4 and a map of each is included in Appendix D. Variation in the number of shortest paths identified is due to a variation in the number of paths initially available between origin and destination points. The number of shortest paths increases with the number of total available paths.

Table 4: Number of paths connecting indicated origin and destination points

	Destination0	Destination1
Origin0	2	9
Origin1	2	3
Origin2	5	3

4.3.2 Entity Creation

Using the unique object identifiers for each road segment from the GIS file, entities are created within the GMOR model. Each segment has four failure entities associated with it, one for each possible damage state the road can experience – none, slight, moderate, and extensive/complete. Repair time and resource dependencies are then added for each damage state for each road. Repair times are generated for each damage state using road segment length information from the GIS model and per-kilometre repair time estimates from the Hazus technical manual (FEMA 2011). A generic resource entity is used for all road segments in this model since it is assumed that standard maintenance crews work to repair the roads as indicated in Section 4.2.

4.3.3 Assumptions

One key assumption made in the modeling process is that all origin points are functional in the immediate aftermath of a disaster. Since it is unknown which point (if any) would actually be accessible in a disaster scenario, this assumption provides an understanding of how repairs propagate from each origin to each destination. Since each path is linked to a specific origin and destination point, assessing the results for the individual paths in the model provides insights into the efficiency of repairs for all possible scenarios, regardless of the functionality of the individual origin points.

Various additional assumptions are made in the generation of this model which may have an effect on the results that are produced as well. These assumptions are primarily related to

repair time and resource issues that are difficult to model and could vary widely in actual disaster scenarios. It is assumed that the uncertainty in repair times included in the model (via normally distributed times indicated in Table 5) account for and accommodate this variability.

Table 5: Mean and standard deviation of normally distributed road repair times per kilometre of road based on level of damage.

Damage	Repair time (days per km)	
	Mean	Standard deviation
None	0	0
Slight	0.9	0.05
Moderate	2.2	1.8
Extensive/complete	21	16

Specifically related to assumptions surrounding repair time are travel and access issues that could impede repair crews and prevent them from quickly reaching and commencing repairs on damaged sections of roadway. Travel time and access are not included in the GMOR model, but it is assumed that these times are considerably smaller than the times necessary to perform repairs on damaged road segments. Further, since some road segments are not included in the model (as shown in Figure 4-4), it is assumed that alternate paths beyond those indicated in Figure 4-4b and Appendix D could provide access for repair crews.

Additionally, ATC-13 documentation indicates that repair times are reported under the assumption that “[u]nlimited resources are available for reconstruction”, which may not realistically be the case (Applied Technology Council 1985). Given that access to the District is already assumed based on the immediate functionality of at least one origin point in the model, this supports the assumption that resources would likely be available by way of these origin points. In addition, while resources may be in short supply immediately following a disaster, the level of damage experienced by the roads considered here is likely not significant enough to

prevent repairs from occurring. Further evidence from recent disasters indicates that, in some cases, materials may be rapidly produced and distributed (Alaska Department of Transportation and Public Facilities 2018), though that falls beyond the scope of this chapter.

4.4 Trials

A beneficial feature in the GMOR model used here is the capability to prioritize resource allocation for performing repairs. This feature allows for the specification of entities (in this case, road segments) that are to be repaired before others. Prioritization may also be randomized, providing insight into how a network might best recover beyond the intuition of modelers. In the initial trials of the model presented here, the prioritization of resource allocation is randomized, so all roads are considered equally in performing repairs. Further trials explicitly prioritize certain groups of road segments over others to determine how the order of repair affects overall network repair time.

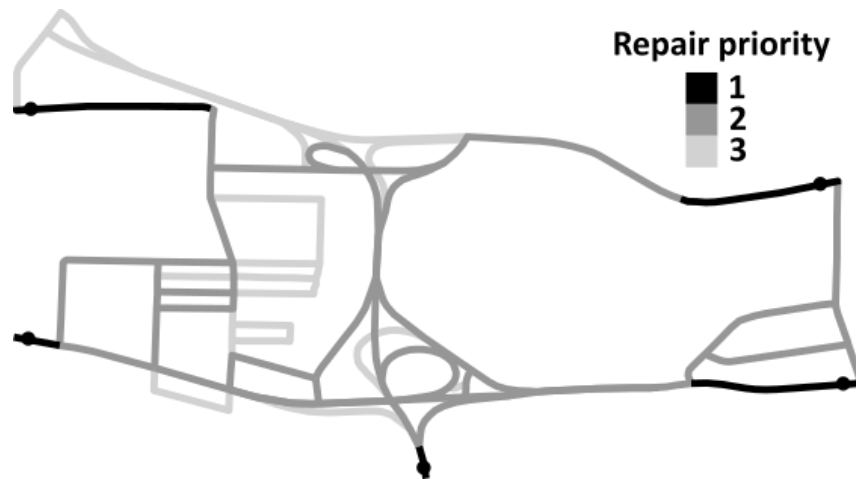


Figure 4-7: Road repair priority levels. Origin and destination points included for reference.

In trials where repair order is specified, three levels of priority are assigned to the various road segments. The list of road segments is split into groups based whether they are included in one of the shortest paths or not. The highest priority roads are those that are connected to an origin or destination point. Next are the segments that are identified as being part of one of the shortest paths. Finally, the road segments that are not included in any shortest path are allocated

resources for repairs. A map highlighting the different priority levels for each road segment is shown in Figure 4-7.

Within each of the differing levels of priority, the repair order of road segments is randomized. That is to say, a road segment included in a path will be repaired before one not included in a path in every trial, but will be randomly assigned a priority among all roads included in a path. This prioritization is not highly complex for the purposes of these trials, but further detail can be included as desired and is discussed in Section 4.6.

4.5 Results

Results are presented here for the two sets of trials identified in Section 4.4. Five hundred trials were generated for each trial type, all based on the initial earthquake scenario identified in the District case study detailed in Chapter 3. Results are shown first by the time it takes for repairs to connect each destination point to any one of the origin points. This repair time reflects the assumption that the road networks into this part of the District are functional. Further results are presented for each origin-destination combination in Table 6, and more detailed results for each path are included in Appendix F.

4.5.1 Randomized Trials

For trials in which no repair order was specified, the average time required to provide a functional path to Destination 0 is 41.6 days, with a standard deviation of 17.9 days. To reach Destination 1, the average repair time is 42.4 days, again with a standard deviation of 17.9 days. The minimum and maximum times required for repairs to reach Destination 0 are 7.1 and 104.1 days, respectively. For Destination 1, the results are similar with a minimum of 6.6 days and maximum of 105.7 days. Histograms for each destination are shown in Figure 4-8.

The average repair times and standard deviations for each origin-destination pair are shown in Table 6, and a box plot for each is included in Appendix E as well.

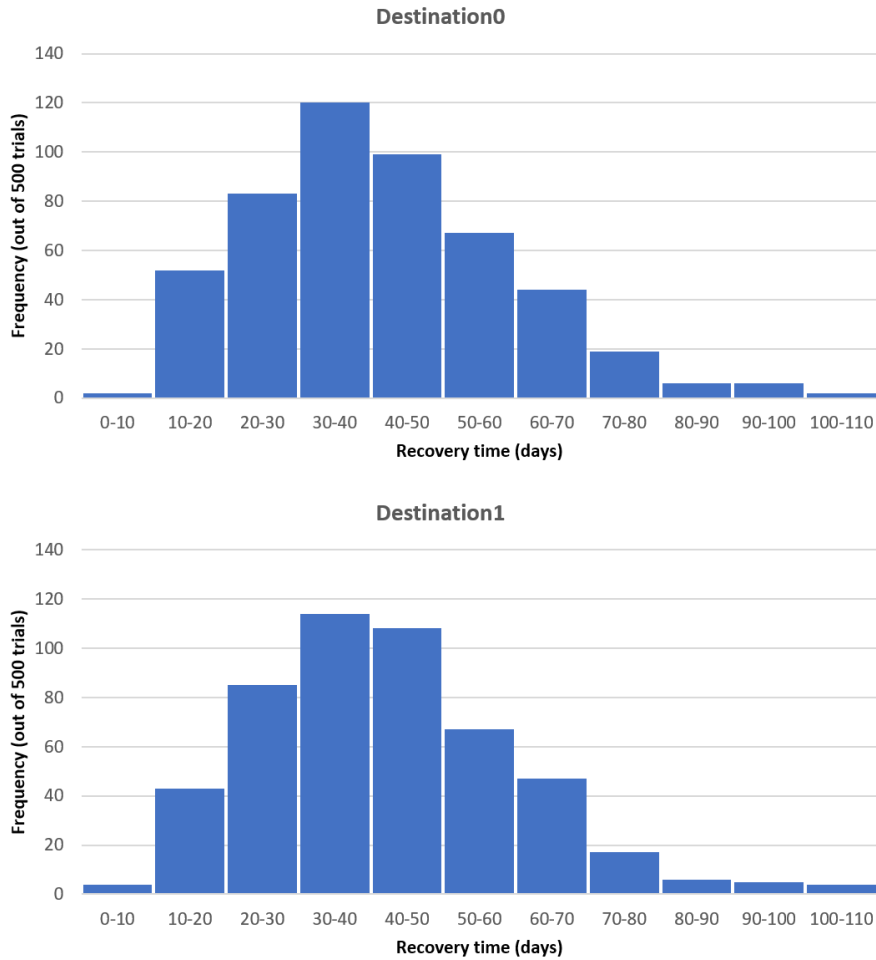


Figure 4-8: Distribution of recovery times for randomized prioritization.

4.5.2 Ordered Trials

For trials in which three levels of priority were modeled as described in Section 4.4, average repair time to reach Destination 0 drops to 26.1 days with a standard deviation of 15.2 days. For Destination 1, the results indicate an average repair time of 27.1 days, with a standard deviation of 15.1 days. A minimum of 1.2 days and maximum of 97.3 days is required to reach Destination 0, while these values are 0.7 days and 86.9 days for Destination 1. Histograms for these results are shown in Figure 4-9. For each origin-destination pair, results are shown in Table 6, and a box plot for each is also included in Appendix E.

Table 6: Mean and standard deviation (σ) of recovery time for origin and destination points. All values given in days.

	Random				Ordered			
	Destination 0		Destination 1		Destination 0		Destination 1	
	Mean	σ	Mean	σ	Mean	σ	Mean	σ
Origin 0	42.3	18.2	43.6	18.3	26.5	15.3	27.7	15.3
Origin 1	46.0	18.5	45.4	18.2	29.9	15.5	29.6	15.5
Origin 2	46.6	18.6	46.5	18.8	30.1	15.5	29.8	15.3

4.5.3 Discussion

As can be clearly seen in the results, prioritizing repairs to road segments that are included in paths connecting origin and destination points drastically improves the repair times needed to reach those points. It is interesting to note, however, that even though the required repair time drops substantially, the standard deviation is reduced by a comparatively small amount. This indicates that individual repair times for specific road segments are subject to roughly the same amount of variability in each set of trials, but the prioritization of repairs shifts the mean to a much lower overall repair time.

In addition, the mean and standard deviation for each origin-destination pair shown in Table 6 demonstrate minimal variation within the types of ordering represented (randomized or specified). This is in part a result of many pairs sharing roads, so once a given road is recovered, multiple pairs recover as well. Further, with randomized ordering, any road may be prioritized over any other, so the paths are recovered in a random order as well. With specified ordering, the roads on which origin and destination points lie are prioritized first. The ordering for the next sets of roads is randomized, so they may recover in any order after that point. If roads that are part of certain paths are consistently ordered before others, results would likely be much less consistent across the origin-destination pairs.

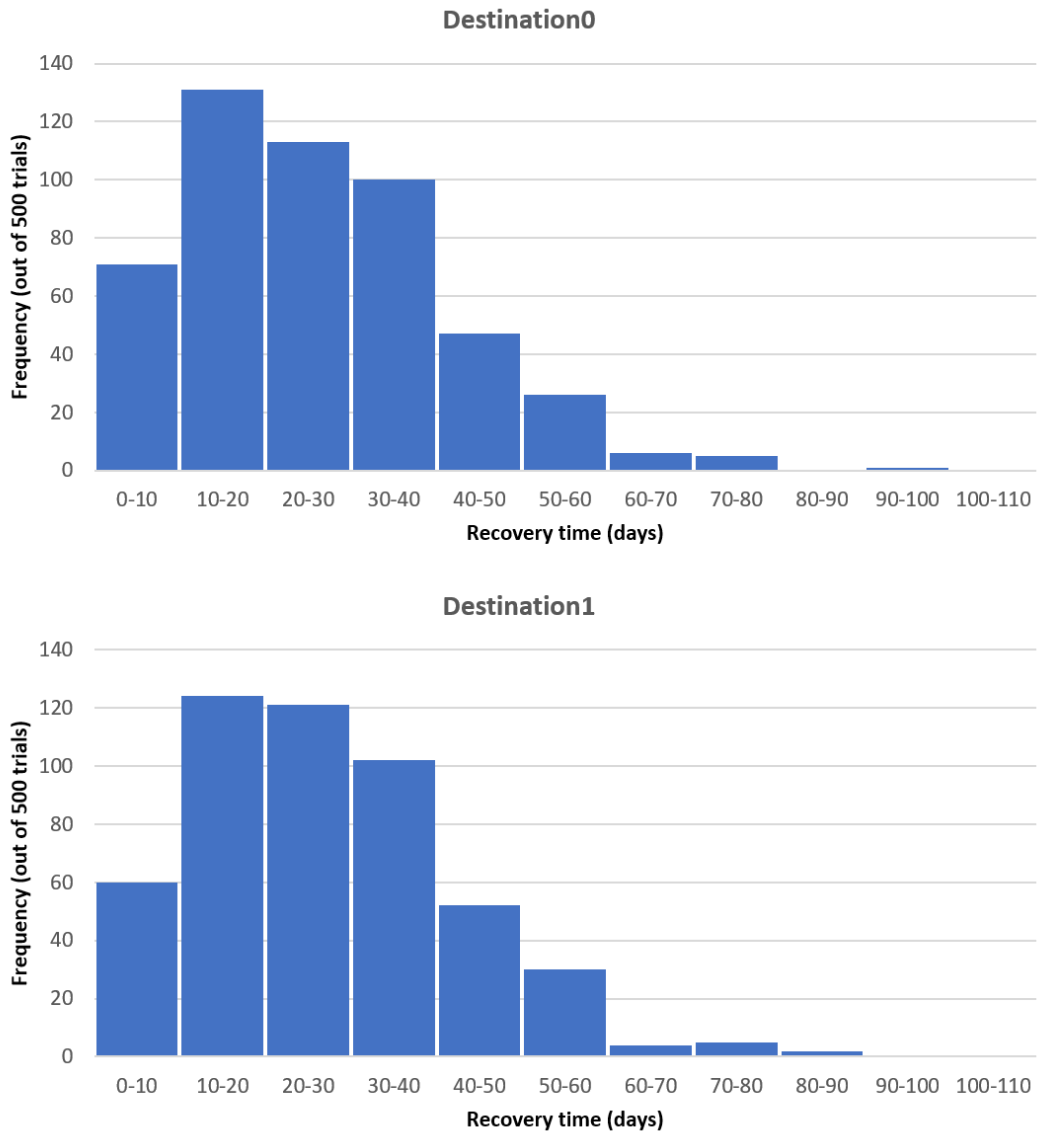


Figure 4-9: Distribution of recovery times for ordered prioritization.

A number of important details must be mentioned when discussing these results. The first is that the repair time shown here is for the complete repair of the included road segments, not simply for access or the ability to traverse a specific road segment. For example, “Slight Damage” and “Moderate Damage” (damage states 2 and 3) in Hazus documentation is characterized by anywhere from a few inches to several inches of settlement in a roadway (FEMA 2011). While this level of damage would certainly require repairs, it would not necessarily prevent access for repair crews, emergency responders, or even residents. As such,

the repair times indicated here are not meant to indicate that no supplies or aid are able to travel through the District in case of a disaster, but that returning to normal roadway function in those areas will take time. Many residents in these neighbourhoods would still likely be able to travel as needed to access essential supplies given the redundancy in the road network.

With regard to emergency services, some of these roads may be used to provide service if they are not significantly damaged. In addition, roads that were marked as being only accessible in one direction in Section 4.3.1 could be traveled on in reverse if necessary to provide supplies or emergency medical care.

The overall repair time for all of the roads in these neighbourhoods is higher than the repair times indicated here for a number of reasons. Some of the roads are not included in this model for simplicity, as indicated in Section 4.2. Further, the key priority in this chapter is to return the roads in this part of the district to normal as quickly as possible. The faster that the efficient travel of goods and services can be restored, the sooner pre-disaster conditions and functionality can be restored to the neighbourhoods involved and the District as a whole.

4.6 Future Considerations

Several options exist to expand and improve on this work in the future. Further optimizing the priority of repairs for roads and paths is one area that can be developed. For example, considering the length, probability of failure, and resulting estimated repair time for specific road segments could provide an opportunity to prioritize repairs of those that are likely to provide the quickest access to the desired origins and destinations. In addition, identifying other key areas within the district could be considered in future modeling scenarios as well. Prioritizing routes to hospitals, shopping centres, or other supply routes, for example, may increase overall repair time in the certain neighbourhoods but improve outcomes for citizens by providing earlier access to critical facilities.

In addition, these trials only cover a small area of a single part of the District, but the same methodology could be extended to larger municipal-scale regions. Specifically, by identifying points of interest or importance at a local scale and performing similar trials for many

areas, key paths within a region may be identified. These paths can then be used to perform larger trials and inform stakeholders for the purposes of coordinating and planning at a regional scale. Further, functions and capabilities within smaller local areas may be available to others nearby, providing the opportunity to improve the efficiency of recovery by sharing resources. Haas (1977) refers to this area as the “invisible city” that surrounds a damaged location.

The Indicator entities introduced in Section 2.3.4 can also be useful for establishing probable accessibility for roads in the district after a disaster. For example, roads experiencing minimal or moderate damage are likely passable, especially if priority is given to emergency services or repair and maintenance crews. Correlating information about roads that are less prone to high levels of failure with roads that connect key areas of a municipality could prove valuable in establishing routes for disaster response activities.

As mentioned previously, the trials run for the purposes of this study do not make any consideration for travel time or access issues related to the process of performing road repairs. It is assumed that additional time required is mitigated by the inclusion of standard deviations for repair times, and that travel time is limited in comparison to actual repair time. In the future, it may be possible to improve accuracy by accounting for impassable roads, crew set up time and resource acquisition. Each of these additions introduces its own variability, so understanding the effect of each on overall recovery time and uncertainty is crucial.

Further benefit could be provided by performing rapid assessment of roads immediately following a disaster to produce quick plans for post-disaster reconstruction. Incorporating observed damage states in the models presented here rather than estimates from simulations would improve the accuracy of results and provide an opportunity to plan for realistic recovery. While the computing resources and time required to run models are significant, improvement in recovery outcomes based on results from those models would likely far outweigh those challenges. That being said, reducing the complexity of models to improve computational efficiency without negatively impacting results should certainly be pursued.

4.7 Conclusion

The work presented here provides an overview of the repair time necessary to connect points of interest within a set of neighbourhoods in the District of North Vancouver after a disaster. Results indicate that prioritizing specific sections of road results in a reduction in the time required to connect these points. The effects of prioritization are highlighted and offer a clear picture of the impact that simple changes may have on recovery at a municipal scale.

This work may be used to support decision-makers and stakeholders as they plan for post-disaster reconstruction or provide insight into where resources should be located or how they should be distributed to prepare before a disaster strikes. Communication with residents in neighbourhoods, recognizing their needs, and understanding the resources and processes that support their well-being should be a critical consideration in developing resilient strategies throughout their communities.

5 Conclusion and future considerations

Natural disasters will continue to occur throughout the world in the coming years, and evidence suggests that their impacts may become even more severe as global populations rise and the effects of climate change become more prominent (Thomas 2017; Coppola 2006). No one can stop these disasters from occurring, but individuals, organizations, and communities can take steps to better prepare themselves for disaster scenarios. Modeling disasters and their effects will help create plans for disaster response and promote faster recovery and reconstruction. The work presented here builds on the capabilities of existing recovery modeling approaches by improving the precision of damage state and recovery time estimates.

Chapter 2 details a methodology for better integrating a probabilistic recovery modeling platform (GMOR) with outputs from existing hazard modeling tools. This integration promotes increased accuracy in correlating levels of damage to infrastructure systems with resource and repair time requirements.

Chapter 3 presents a case study of the effects of a hypothetical earthquake on the functionality and restoration of water, wastewater, power, and road systems in the District of North Vancouver. Results from this study indicate that recovery times for water and wastewater systems are on average significantly lower than those of power and road networks. In addition, power and road network repair times are subject to a high level of variability, so communities must be prepared to respond to a wide variety of outages and lack of functionality in these systems.

Chapter 4 expands on the work presented in Chapter 3 and offers a focused view of part of the road network within the District of North Vancouver. The road segments considered in this chapter connect the District to external locations that are critical for providing resources for the District's recovery. The prioritization of resource allocation highlighted in this chapter show the importance of properly distributing repair resources after a disaster to expedite recovery.

Many options exist for building and improving on this work to further suit the needs of a wide variety of communities and organizations. The focus here is primarily on the physical

structures that exist within municipalities, which are important to sustaining the health and well-being of residents. That being said, considering the psychosocial and other needs of communities is essential as well. Too often, physical structures and social strategies are treated separately, but they exist in mutually supportive roles whose interactions should be more clearly researched and understood. Two communities with exactly the same infrastructure systems subject to the same disaster may have drastically different goals and priorities, which must be considered and respected when planning for recovery.

In addition, other resilient strategies must be considered in future scenarios. This work touched briefly on the importance of resource prioritization in improving recovery times, but other actions should be modeled in the future as well. These could include increasing resource availability (such as adding repair crews or materials), decreasing likelihood of damage after a disaster (by constructing stronger facilities or building in less risky areas), increasing redundancy (by adding additional power production facilities in a community), or further improving damage and recovery time estimates to better understand what happens within a community or organization during and immediately following a disaster.

As it stands, this work serves as a framework for broader case studies and provides guidance for establishing parameters and scenarios for resilience and recovery assessment. Recovery and restoration are fields that still require much research, but it is hoped that the work presented here bridges a gap in understanding and provides capabilities that are useful for improving outcomes after disaster for communities and organizations in the future.

References

- Alaska Department of Transportation and Public Facilities. 2018. "Earthquake Damage Assessment Updates." 2018. <http://dot.alaska.gov/earthquake2018/>.
- American Lifelines Alliance. 2001. "Seismic Fragility Formulations for Water Systems." https://www.americanlifelinesalliance.com/pdf/Part_2_Appendices.pdf.
- Anbazhagan, Panjamani, Sushma Srinivas, and Deepu Chandran. 2012. "Classification of Road Damage Due to Earthquakes," 425–60. <https://doi.org/10.1007/s11069-011-0025-0>.
- Applied Technology Council. 1985. "ATC-13: Earthquake Damage Evaluation Data for California." Redwood City, CA.
- Berke, Philip R, Jack Kartez, and Dennis Wenger. 1993. "Recovery after Disaster : Achieving Sustainable Development , Mitigation and Equity" 17 (2).
- Bocci, Maurizio, Andrea Grilli, Fabrizio Cardone, Gilda Ferrotti, Maurizio Bocci, Andrea Grilli, Fabrizio Cardone, and Gilda Ferrotti Full-. 2014. "Full-Depth Reclamation for the Rehabilitation of Local Roads : A Case Study" 8436. <https://doi.org/10.1080/10298436.2012.657196>.
- Bragado, Alejandro Diaz-Delgado. 2016. "Downtime Estimation of Lifelines after an Earthquake."
- Bristow, David N., and Alexander H. Hay. 2017. "Graph Model for Probabilistic Resilience and Recovery Planning of Multi-Infrastructure Systems." *Journal of Infrastructure Systems* 23 (3): 04016039. [https://doi.org/10.1061/\(ASCE\)IS.1943-555X.0000338](https://doi.org/10.1061/(ASCE)IS.1943-555X.0000338).
- Bristow, David N. 2019. "How Spatial and Functional Dependencies between Operations and Infrastructure Leads to Resilient Recovery." *Journal of Infrastructure Systems* 25 (2): 1–8. [https://doi.org/10.1061/\(ASCE\)IS.1943-555X.0000490](https://doi.org/10.1061/(ASCE)IS.1943-555X.0000490).
- Cassottana, Beatrice, Lijuan Shen, and Loon Ching Tang. 2019. "Modeling the Recovery Process: A Key Dimension of Resilience." *Reliability Engineering and System Safety* 190 (April). <https://doi.org/10.1016/j.res.2019.106528>.
- Choi, Juyeong, Abhijeet Deshmukh, and Makarand Hastak. 2016. "Increase in Stress on

- Infrastructure Facilities Due to Natural Disasters.” *International Journal of Urban Sciences* 20 (May): 77–89. <https://doi.org/10.1080/12265934.2016.1170626>.
- Coppola, Damon P. 2006. *Introduction to International Disaster Management*. Burlington: Elsevier Inc.
- DNV. 2015. “When the Ground Shakes : A Plain Language Companion Study.” <https://www.dnv.org/sites/default/files/edocs/when-the-ground-shakes.pdf>.
- Donahue, Amy K., Catherine C. Eckel, and Rick K. Wilson. 2014. “Ready or Not? How Citizens and Public Officials Perceive Risk and Preparedness.” *American Review of Public Administration* 44 (4 SUPPL.). <https://doi.org/10.1177/0275074013506517>.
- Donev, Valentin, and Markus Hoffmann. 2018. “Optimisation of Pavement Maintenance and Rehabilitation Activities , Timing and Work Zones for Short Survey Sections and Multiple Distress Types Zones for Short Survey Sections and Multiple Distress Types.” *International Journal of Pavement Engineering* 0 (0): 1–25. <https://doi.org/10.1080/10298436.2018.1502433>.
- Duffey, Romney B. 2019. “Power Restoration Prediction Following Extreme Events and Disasters.” *International Journal of Disaster Risk Science* 10 (1): 134–48. <https://doi.org/10.1007/s13753-018-0189-2>.
- European Commission. 2019. “RAPID-N: Rapid Natech Risk Assessment Tool.” 2019. <http://rapidn.jrc.ec.europa.eu/>.
- FEMA. 2011. “Hazus – MH 2.1 Earthquake Model Technical Manual.” Washington, D.C. https://www.fema.gov/media-library-data/20130726-1820-25045-6286/hz mh2_1_eq_tm.pdf.
- Ganin, Alexander A., Maksim Kitsak, Dayton Marchese, Jeffrey M. Keisler, Thomas Seager, and Igor Linkov. 2017. “Resilience and Efficiency in Transportation Networks.” *Science Advances* 3 (12): 1–9. <https://doi.org/10.1126/sciadv.1701079>.
- Gao, Xueying, and Di Sun. 2012. “Assessment of Road Damage and Schedule Study of Road Repair after Earthquake.” In *World Automation Congress, 2012*.

- Haas, J E, R W Kates, M J Bowden, and D Amaral. 1977. *Reconstruction Following Disaster*. Environmental Studies Series. MIT Press.
<https://books.google.ca/books?id=ZxJ2QgAACAAJ>.
- Haimes, Yacov Y. 2009. “On the Complex Definition of Risk: A Systems-Based Approach.” *Risk Analysis* 29 (12): 1647–1654. <https://doi.org/10.1111/j.1539-6924.2009.01310.x>.
- Hawa, Abideng, Danupon Tonnayopas, Woraphot Prachasaree, and Pichai Taneerananon. 2013. “Development and Performance Evaluation of Very High Early Strength Geopolymer for Rapid Road Repair.”
- He, Fei, and Johnpaul Nwafor. 2017. “Gas Pipeline Recovery from Disruption Using Multi-Objective Optimization.” *2017 IEEE International Symposium on Technologies for Homeland Security, HST 2017*, 1–6. <https://doi.org/10.1109/THS.2017.7943495>.
- Howard, Isaac L, Jesse D Doyle, James Michael, Hemsley Jr, L Gaylon, L Allen Cooley Jr, Isaac L Howard, et al. 2014. “Emergency Paving Using Hot-Mixed Asphalt Incorporating Warm Mix Technology” 8436. <https://doi.org/10.1080/10298436.2012.721549>.
- Hu, Xiao Bing, Ming Wang, Tao Ye, and Peijun Shi. 2016. “A New Method for Resource Allocation Optimization in Disaster Reduction and Risk Governance.” *International Journal of Disaster Risk Science* 7 (2): 138–50. <https://doi.org/10.1007/s13753-016-0089-2>.
- Janani, L, Raunak Kumar Dixit, V Sunitha, Samson Mathew, and Samson Mathew. 2019. “Prioritisation of Pavement Maintenance Sections Deploying Functional Characteristics of Pavements.” *International Journal of Pavement Engineering* 0 (0): 1–8.
<https://doi.org/10.1080/10298436.2019.1567923>.
- Journey, J M, F Dercole, D Mason, M Westin, J A Prieto, C L Wagner, N L Hastings, S E Chang, A Lotze, and C E Ventura. 2015. “A Profile of Earthquake Risk for the District of North Vancouver, British Columbia.” <https://doi.org/10.4095/296256>.
- Kolmogorov, A N, and A T Bharucha-Reid. 1956. *Foundations of the Theory of Probability*. https://www.york.ac.uk/depts/maths/histstat/kolmogorov_foundations.pdf.
- Lempert, A A, D N Sidorov, A V Zhukov, and G L Nguyen. 2016. “A Combined Work Optimization Technology under Resource Constraints with an Application to Road Repair”

- 77 (11): 1883–93. <https://doi.org/10.1134/S0005117916110011>.
- Li, Shuanglin, and Kok Lay Teo. 2018. “Post-Disaster Multi-Period Road Network Repair : Work Scheduling and Relief Logistics Optimization.” *Annals of Operations Research*. <https://doi.org/10.1007/s10479-018-3037-2>.
- Loggins, Ryan A, and William A Wallace. 2015. “Rapid Assessment of Hurricane Damage and Disruption to Interdependent Civil Infrastructure Systems.” *Journal of Infrastructure Systems* 21 (4): 1–12. [https://doi.org/10.1061/\(ASCE\)IS.1943-555X.0000249](https://doi.org/10.1061/(ASCE)IS.1943-555X.0000249).
- Lubashevskiy, Vasily, Taro Kanno, and Kazuo Furuta. 2013. “Algorithm for Resource Redistribution Required for Recovery of Society after Large Scale Disasters.” <https://doi.org/10.1142/S021952591450026X>.
- Miles, Scott B. 2018. “Participatory Disaster Recovery Simulation Modeling for Community Resilience Planning.” *International Journal of Disaster Risk Science* 9 (4): 519–29. <https://doi.org/10.1007/s13753-018-0202-9>.
- Onuma, Hiroki, Kong Joo, and Shunsuke Managi. 2017. “Household Preparedness for Natural Disasters : Impact of Disaster Experience and Implications for Future Disaster Risks in Japan.” *International Journal of Disaster Risk Reduction* 21 (July 2016): 148–58. <https://doi.org/10.1016/j.ijdr.2016.11.004>.
- Ouyang, Min. 2014. “Review on Modeling and Simulation of Interdependent Critical Infrastructure Systems.” *Reliability Engineering and System Safety* 121: 43–60. <https://doi.org/10.1016/j.res.2013.06.040>.
- Robinson, Tom R, and Tom R Robinson. 2018. “Road Impacts from the 2016 Kaikōura Earthquake : An Analogue for a Future Alpine Fault Earthquake ? Road Impacts from the 2016 Kaikōura Earthquake : An Analogue for a Future Alpine Fault Earthquake ?” *New Zealand Journal of Geology and Geophysics* 61 (3): 403–11. <https://doi.org/10.1080/00288306.2018.1470539>.
- Rodríguez, Havidán, William Donner, and Joseph E Trainor, eds. 2018. *Handbooks of Sociology and Social Research Handbook of Disaster Research*. 2nd ed. Springer International Publishing. <http://www.springer.com/series/6055>.

Rodríguez, Havidán, Enrico L. Quarantelli, and Russell R. Dynes, eds. 2007. *Handbook of Disaster Research*. New York: Springer Science+Business Media, LLC.

Rubin, Claire B, Martin D Saperstein, and Daniel G Barbee. 1985. “Community Recovery from a Major Natural Disaster.”

Shaw, Rajib, ed. 2014. *Disaster Recovery: Used or Misused Development Opportunity*. Tokyo: Springer. <https://doi.org/https://doi.org/10.1007/978-4-431-54255-1>.

Statistics Canada. 2017. “North Vancouver, DM [Census Subdivision], British Columbia and Greater Vancouver, RD [Census Division], British Columbia (Table). Census Profile.” In *2016 Census. Statistics Canada Catalogue No. 98-316-X2016001*. Ottawa.

Thomas, Vinod. 2017. *Climate Change and Natural Disasters*. London and New York: Routledge.

Zhao, Chen, Nan Li, and Dongping Fang. 2018. “Criticality Assessment of Urban Interdependent Lifeline Systems Using a Biased PageRank Algorithm and a Multilayer Weighted Directed Network Model.” *International Journal of Critical Infrastructure Protection* 22: 100–112. <https://doi.org/10.1016/j.ijcip.2018.06.002>.

Appendix A: Mutually Exclusive Failure Dependency Map Creation

A.1 Introduction

Between the dependency map shown in Figure 2-1 in Section 2.2.1 and the one shown in Figure 2-3 in Section 2.3 are many intermediate steps that provide the structure for the integration of mutually exclusive failure states in GMOR. These steps are outlined here to provide clarity and describe the process of adding this methodology to GMOR.

A.2 Dependency Map Creation

A dependency map is a visual representation of the functions, processes, resources, and other components that are required for a specific component to function within a system. In a GMOR model, each of the pieces represented in a dependency map is initially held in a text file that provides GMOR with the information needed to run a simulation. The types of files used and their functionality is described in more detail in Appendix C. As such, the visual dependency map is not used directly in GMOR but is useful to understand the structure of models that are produced.

A.3 Basic Entity Structure

A basic GMOR entity is shown in Figure A-1 with its dependencies included. A description of the logic gates used and their functionality is described Section 2.2.1 and is therefore not included here.

The Failure box in Figure A-1 has an associated probability of occurrence that is defined in the GMOR model and requires a unique Repair Time provided by a specific Resource in order to restore the Entity to its proper functionality.

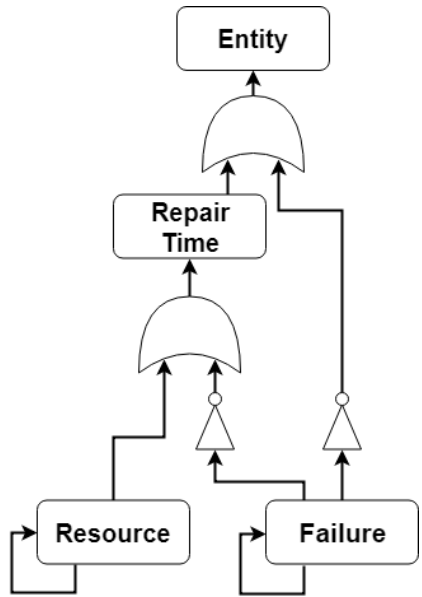


Figure A-1: Basic structure of a single entity in GMOR with repair time, failure, and resource dependencies shown.

A.3.1 Duplicating Entities

The overarching process for producing models with mutually exclusive failure states involves creating individual entities to serve as indicators of the functionality of components in response to each possible failure state. Each of these entities has its own associated repair time and probability of failure, but shares a resource with all other entities. Duplicated entities with unique repair times, unique failure states and probabilities, and a shared resource are shown in Figure A-2.

A.3.2 Recovery Indicators

To show that a specific failure state has not occurred or that the required repair time has passed for an experienced failure, the individual entities are relabeled as indicators which the overall entity of interest is dependent on, as shown in Figure A-3. In addition, a connection is made between Failure 1 and the OR gate for Indicator 2. This connection helps ensure that failures are represented as mutually exclusive in the model. That is, when Failure 1 occurs (takes on a value of 1), Indicator 2 shows a 1 as well, indicating that Failure 2 has not occurred, regardless of the

actual initial value of Failure 2 in the simulation. This process is described in more detail in Section 2.3.

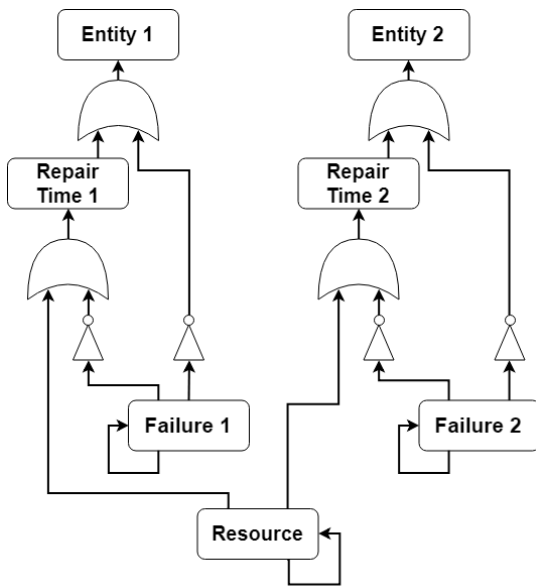


Figure A-2: New entity with unique repair time, unique failure states, and shared resource entities.

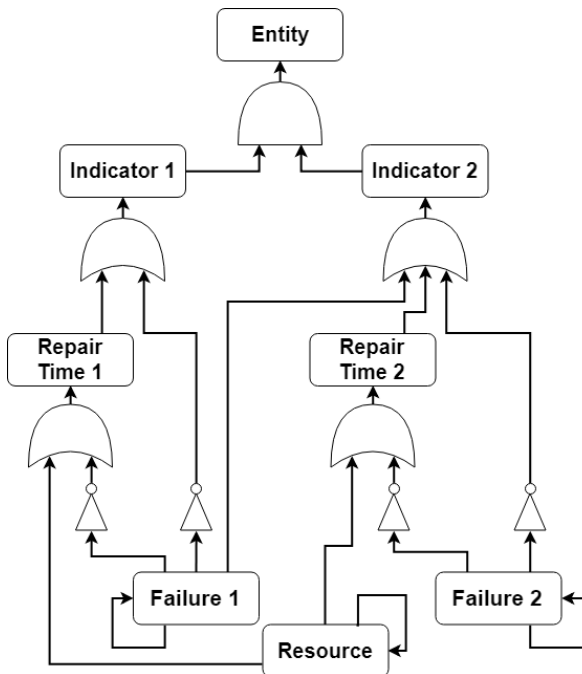


Figure A-3: Indicator entities added to the dependency map, as well as a connection between Failure 1 and the OR gate for Indicator 2.

A.3.3 Additional Failure State

To match the structure of the dependency map shown in Figure 2-3, an additional failure state needs to be added to the model. This is achieved by adding an additional indicator entity to the model and connecting it to the other two entities. An updated dependency map is shown in Figure A-4. Note the additional link from Failure 1 to the OR gate for Indicator 3, as well as the link from Failure 2 to the OR gate for Indicator 3.

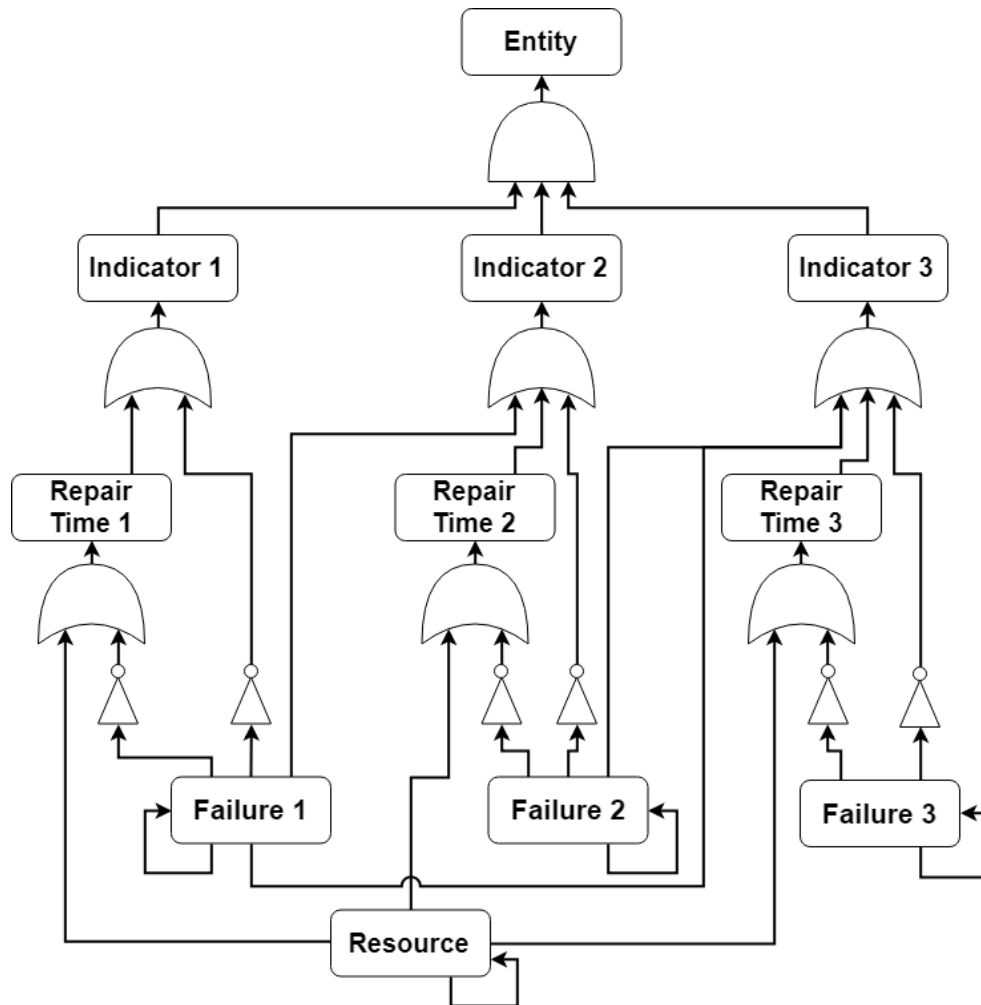


Figure A-4: Dependency map for entity with three possible failure states.

If additional entities are added, the same process is followed. Lower numerical value Failure entities are connected to the OR gates of Indicator entities to ensure that only one failure at a time is represented in the model.

A.3.4 Resource Allocation

The dependency maps shown in Figure A-1 and Figure A-4 are for a single entity with a dedicated resource. In a larger system, however, resources may be shared among many entities. As a result, GMOR needs a means by which to allocate resources effectively and prioritize the repair of certain entities over others. Connecting resources directly to Repair Time entities increases the complexity of the GMOR model and complicates the allocation of resources. As a result, the resource is instead applied to an additional set of entities that contain the entire repair process. This allows for the order of repair to be specified for each entity in the GMOR model as described in Section 2.3.2. The final dependency map for this entity is shown in Figure A-5.

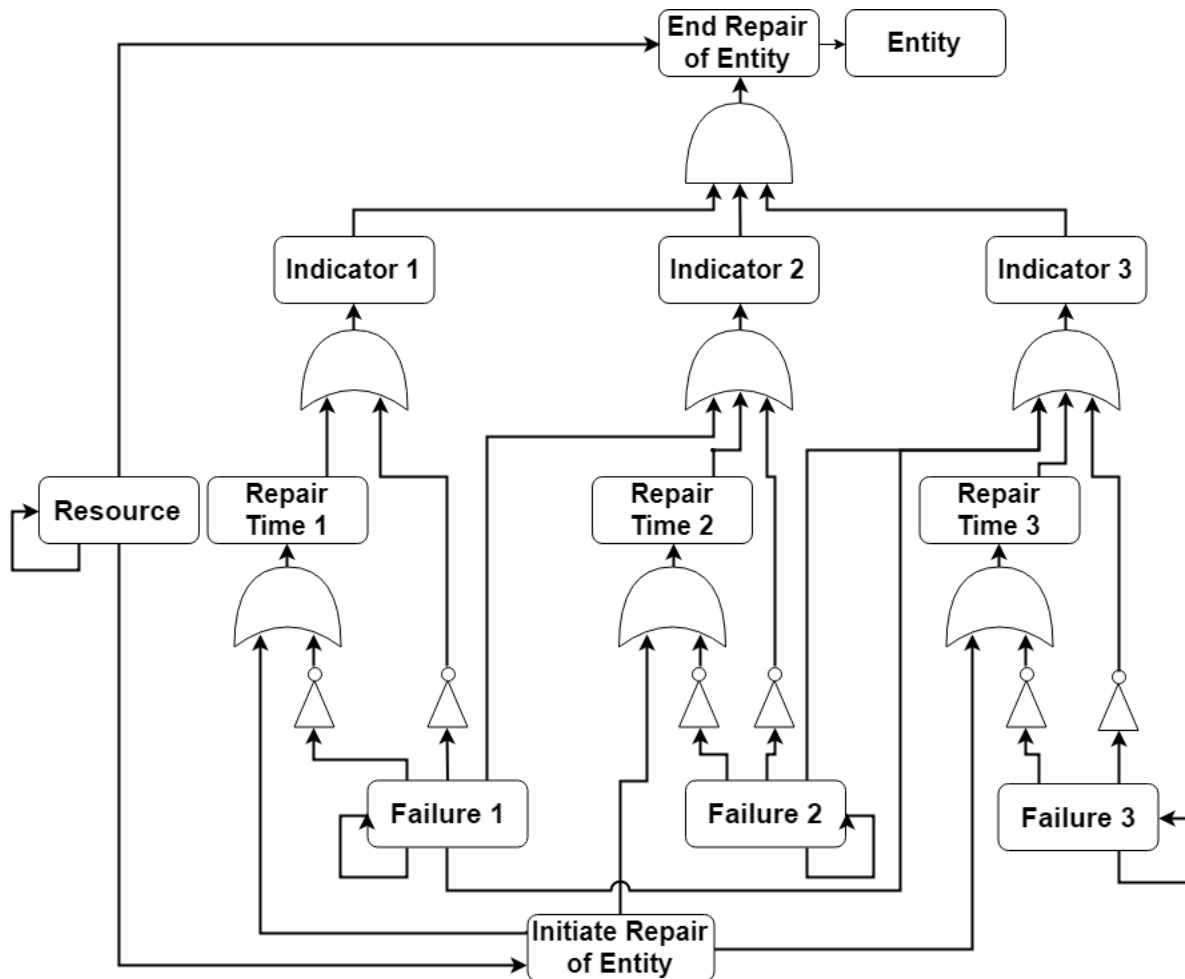


Figure A-5: Full dependency map for entity with three possible mutually exclusive failure states.

Appendix B: Supplemental Information for Chapter 3

B.1 Water Distribution and Wastewater Collection Networks

Breaks and leaks in water distribution and wastewater collection pipelines are modeled in Hazus by the federal government partner for each individual pipe segment. In this model, the District is divided into neighbourhood zones and the number of expected breaks and leaks is tallied in each zone. The failure of the pipes in each zone is set to 1 and then the variation in recovery time in the zone is estimated based on a repair time distribution as follows.

B.1.1 Failure and repair time distribution

From the Hazus Technical Manual (FEMA 2011) the repair times of pipes per crew are the following for a 16 hour shift:

		Small pipe	Large pipe	Value used
Repair time per:	Leak	4 hours	6 hours	7.5 hours
	Break	8 hours	12 hours	15 hours

Since we do not know the pipe diameters the average of these values is used and they are adjusted upward to account for the shift length relative to the hours in the day, giving 7.5 hours per leak per crew and 15 hours per break per crew.

These quantities are taken as the mean repair times for leaks and breaks respectively. While nearly all other repairs are modeled as normal distributions in Hazus, no standard deviation is available for pipe repair. Due to this unavailability of data the standard deviation is estimated from the coefficient of variation (COV):

$$COV=\sigma/\mu$$

Ranges of the COV for other repairs in the Hazus documentation vary from approximately 0.25 to 0.75. Here a COV of 0.5 is used. The resulting distribution for pipe leak and break repair is estimated as the following for a crew of 4:

Repair Task	Mean (Days)	Standard Deviation (Days)
Leak	0.313	0.156
Break	0.625	0.313

Each zone of the model comprises a given number of pipes whose number of leaks and breaks are modeled in Hazus (by the federal government partners), hence an overall distribution for repair of water or wastewater pipes in each zone can be computed as the sum of normal distributions. Estimates of the number of leaks and breaks can be converted into estimates of repair times as follows. Given n leaks and m breaks in a prescribed area, the repair time follows a normal distribution such that:

$$\mu = f(n\mu_L + m\mu_B) \quad \sigma^2 = f(n\sigma^2 + m\sigma^2)$$

where $f=1$ is the fraction of leaks that need to be repaired. The value of 1 is used as it is assumed that the estimates for failure rates produced by Hazus are based on observed leaks from historical cases that were used to develop Hazus methodology.

Work crews in the model are assigned to a neighbourhood of the District and they fix all leaks and breaks in that region, then move onto the next region. As such, the more leaks and breaks in a prescribed area of the District, the longer time (on average) that a work crew is required in that area. The order in which workers move from neighbourhood to neighbourhood is randomized in the GMOR model due to a lack of a better alternative.

B.1.2 Workforce resource use per repair activity

There are approximately $n=4$ teams of 4 workers in the District for the water distribution and wastewater collection networks. Each team is modeled to work in isolation, so each repair

activity (for breaks or leaks) uses a quarter of the labour resource under normal operations – this fraction is called the *effort*.

There is a probability, p (provided by the federal government's model) that the availability of crews is halved following the events of the earthquake. It is possible, then, to calculate the expected value of the effort each repair will take as:

$$E[effort] = p \frac{2}{n} + (1 - p) \frac{1}{n} = \frac{1 + p}{n}$$

For this model the probabilities and resulting efforts are:

Network	p (%)	E[Effort]
Water	6.6	0.267
Wastewater	6.6	0.267

B.2 Water and wastewater facilities

Water quality and wastewater treatment are not included in the model. Water supply is made possible by a set of transmission facilities and a largely gravity fed system. For the transmission pumping facility, the recovery times from Hazus are weighted by the Hazus computed probabilities of damage, resulting in:

$$\sim N(\mu = 2.83 \text{ days}, \sigma = 1.34 \text{ days})$$

B.3 Roads

Like water and wastewater systems, roadways are divided into neighbourhood zones in the District, so a similar procedure is followed. Repair times for roadways are taken to follow normal distributions based on their state of damage as indicated in Hazus documentation. The probability of each damage state for individual roadway segments are weighted by their fraction of the total roadway length in the neighbourhood. All segment damage state values are then

summed to represent the average probability of each damage state to the roadway network as a whole within the neighbourhood.

The equation for the overall probability of damage state j for overall neighbourhood road network k based on probabilities for individual road segments i is as follows, where L represents road length:

$$p(k_j) = \sum_{i=1}^i \frac{L_i}{L_k} * p(i_j)$$

The probability of occurrence for each damage state is computed by Hazus and provided by the federal partners.

Weighting and summing the probabilities of occurrence for each damage state and roadway segment within a neighbourhood can lead to extreme outliers being represented in estimates of recovery time. For example, if a neighbourhood consists of one hundred one-kilometre long roadway segments, each with a one percent chance of extensive (DS-5) damage in an earthquake scenario, the overall probability of the entire road network in that neighbourhood experiencing extensive damage will be represented as one percent based on the equation above. In hundreds of trials, that will result in multiple scenarios modeled where all one hundred kilometres of road are completely destroyed. Though this is highly unlikely in reality due to the area covered by a neighbourhood of this size, the model could produce a repair time estimate of ten or more years, given the average required repair time of over twenty days per kilometre of extensively damaged road. These situations are acknowledged and discussed further in Chapter 3.

B.4 Electricity Distribution

Power distribution is divided into neighbourhood zones as well, so a similar procedure to the road networks is followed. There are some differences due to data availability, however. Resource constraints and repair times are not applied per usual using Hazus or other empirical data. Instead, the population weighted recovery time is calibrated to federal partner figures

(68.1% chance of a 6 month failure to 75,000 customers). From this it follows that the mean recovery time in zone i can be estimated by:

$$\tau_i = Population_i f_\tau$$

where f_τ is found by solving the following equation iteratively using a goal seek of 6 months:

$$E[t_{recovery}] = \frac{\sum p_i Population_i f_\tau}{\sum Population_i} = 6$$

where p_i is the chance of failure in zone i . It is assumed that the chance of failure is proportional to the population of each zone, such that:

$$E[p_{failure}] = \sum p_i Population_i = 68.1\% * 75,000$$

A COV=0.5 is used as per other lifelines.

B.5 Outside scenario scope

- It is assumed at that there is an adequate supply of materials and equipment available for repair/replacement
- Water reservoirs and storage are unaffected
- Lifeline bridges to the municipality are not assumed to fail.

Appendix C: Example GMOR files

The three main kinds of files that GMOR uses to gather information are called the “transform”, “scenario”, and “order” files. Examples of the formatting for each are shown in the following sections. Note that ellipses (...) indicate that properties of many entities are not shown. This was to simplify the files for inclusion here, leaving only the names of entities rather than all of their associated parameters.

C.1 Transform File

The transform file holds information about entities and their dependencies in the GMOR model as shown here with annotations on the right:

```
1 [{
2     "name": "Road0", //Name of the entity in the
3     "shp_path": "Project_folder", //model. This entity was
4     "shp_file": "Shapefile_name.shp", //generated from a spatial
5     "root_name": "Road", //join using the shapefile
6     "ent_type": "function", //indicated here. Root name,
7     "parent": "system", //type, and parent all direct
8     "dependencies": ["End Repair of Road0"], //GMOR in how to treat this
9     "obj_ids": ["1"] //entity. Dependencies are
10 }, { //assigned based on the mutually
11     "name": "End Repair of Road0", //exclusive dependency map. The
12     ... // "object ID" correlates the
13 }, { //GMOR entity to the shapefile
14     "name": "I-1 Road0", //entity. Additional entities are
15     ... //created following the structure
16 }, { //of the mutually exclusive
17     "name": "Repair Time of Road DS-1 0", //dependency map. "I-2...", "Repair
18     ... //Time of Road DS-2...", etc, so
19 }, { //only a limited number are shown
20     "name": "Failure of Road DS-1 0", //here. Using a spatial join to a
21     ... //shapefile allows GMOR to create
22 }, { //many entities at once. For example,
23     "name": "Initiate Repair of Road0", //only "Road0" and its associated
24     ... //entities are shown here, but any
25 }, { //number of road entities that are
26     "name": "Road Repair Workforce", //included in the shapefile could be
27     ... //generated, along with all of their
28 }, { //associated entities.
29     "name": "User0", //This entity was generated from
30     ... //a path join. A path join uses
31     "dependencies": [{ //a graph model of the road network
32         "OR": [{ //generated from a shapefile and a list
```

```

33     "OR": [{
34         "AND": ["Source0", {
35             "OR": [{
36                 "AND": ["Road0", "Road1"]
37             }, {
38                 "AND": ["Road2"]
39             }]}]}]
40     },
41     "obj_ids": ["4"],
42     "shp_path": "SourceAndUser",
43     "shp_file": "SourceAndUser.shp"
44 }, {
45     "name": "Source0",
46     ...
47 }, {
48     "name": "Power",
49     ...
50     "dependencies": [{
51         "OR": [{
52             "NOT": ["Failure of Power"]
53             }, "Repair Time of Power"]
54         }
55     ],
56     "obj_ids": []
57 }, {
58     "name": "Power Repair Crew",
59     ...
60 }, {
61     "name": "Failure of Power",
62     ...
63 }, {
64     "name": "Repair Time of Power",
65     ...
66     }
67 ]
68 }
69]

```

//of road connections to find paths
//between selected origin (source) and
//destination (user) points. These paths
//consist of road entities that connect
//the desired points of interest. Here it
//is shown that User0 can reach Source0
//via a combination of Road0 and Road1,
//or Road2 on its own. Once Source0 and
//one of those paths is functional,
//User0 becomes functional as well.

//This entity has no connection to a
//shapefile or any other external file.
//It exists only within the GMOR model
//and therefore has no associated
//"object ID".

C.2 Scenario File

The scenario file holds information about the probability of failure and required repair time for the entities within the model. Note that in a full scenario file, all of the entities from the transform file would be included with their parameters shown. They are eliminated here for the sake of simplicity.

```

1 {"Road 0": {
2     "state_type": "deterministic", //The "state_type" and
3     "time_type": "single", // "time_type" parameters
4     "time": 0.0, //tell GMOR how to treat
5     "state": 1 //entities in this file.

```

```

6 }, //The "time" parameter is a
7 "Failure of Road DS-1 0": { //delay for the model to
8   "state_type": "probabilistic", //wait a certain amount of
9   "time_type": "single", //time once dependencies are
10  "prob_occurrence": 0.5, //in tact before showing an
11  "time": -1.0 //entity as functional.
12 }, // "prob_occurrence" is the
13 "Initiate Repair of Road0": { //probability that the indicated
14   "efforts": { //failure will occur while the
15     "Road Repair Workforce": { //model runs.
16       "effort_type": "single", // "efforts" show the resources
17       "effort": 1.0 //that are required for an
18     } //entity to return to
19   } //functionality.
20 "Repair Time of Road DS-2 0": { //The "time_type": "normal" here
21   "state_type": "deterministic", //shows that the repair time
22   "time_type": "normal", //for this entity is normally
23   "state": 1, //distributed with the indicated
24   "mean": 0.09, //"mean" and "std" values.
25   "std": 0.01
26   }
27 }

```

C.3 Order file

The order file lists the resources that entities in the model rely on as well as the priority in which resources are assigned to entities in the model.

```

1 {
2   "Road Repair Workforce": { //Three entities (Road0, Road1, and Road2)
3     "Initiate Repair of Road0": 1, //depend on this resource for repair. The
4     "Initiate Repair of Road1": 0, //lower the indicated value, the earlier the
5     "Initiate Repair of Road2": 1 //repair will commence. In this example, Road1
6   }, //will be repaired first, then Road0 and Road2
7   "Power Repair Crew": { //will be randomly assigned. The resource for
8     "Repair Time of Power": 0 //the Power entity is not shared with any
9   } //other entities, so its repair commences
10 } //immediately

```

Appendix D: Maps of paths connecting origin and destination points for the road network identified in Chapter 4

The maps shown here demonstrate the various paths used to connect the origin and destination points identified in the central part of the District of North Vancouver as identified in Chapter 4. A map of the simplified road network discussed in Section 4.3.1 and the selected origin and destination points is shown in Figure D-1.

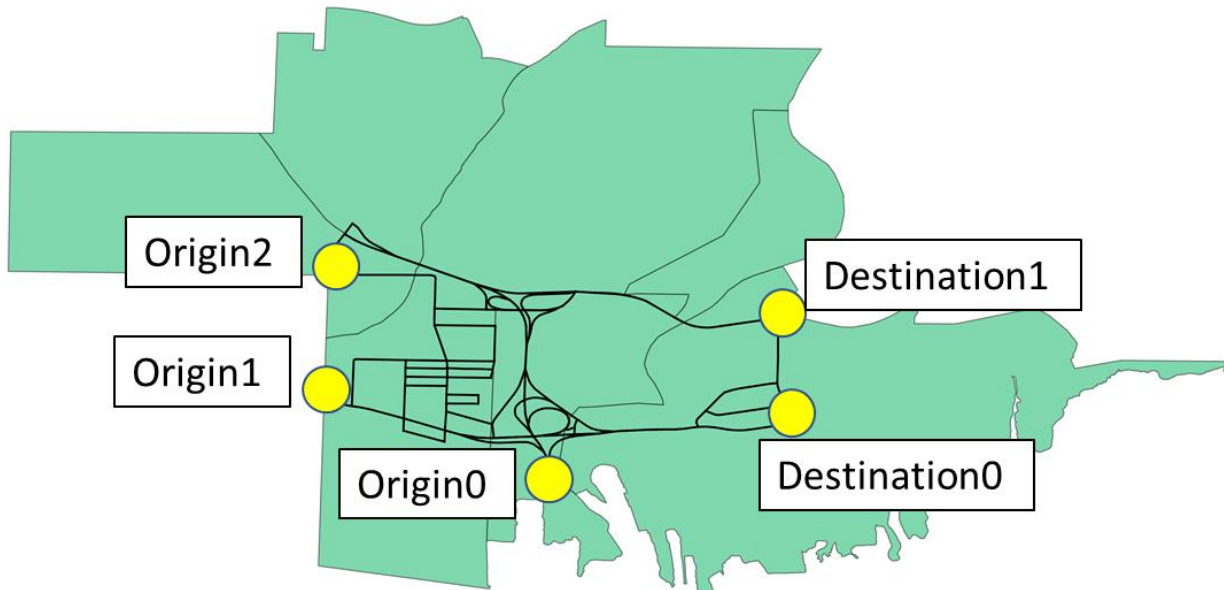
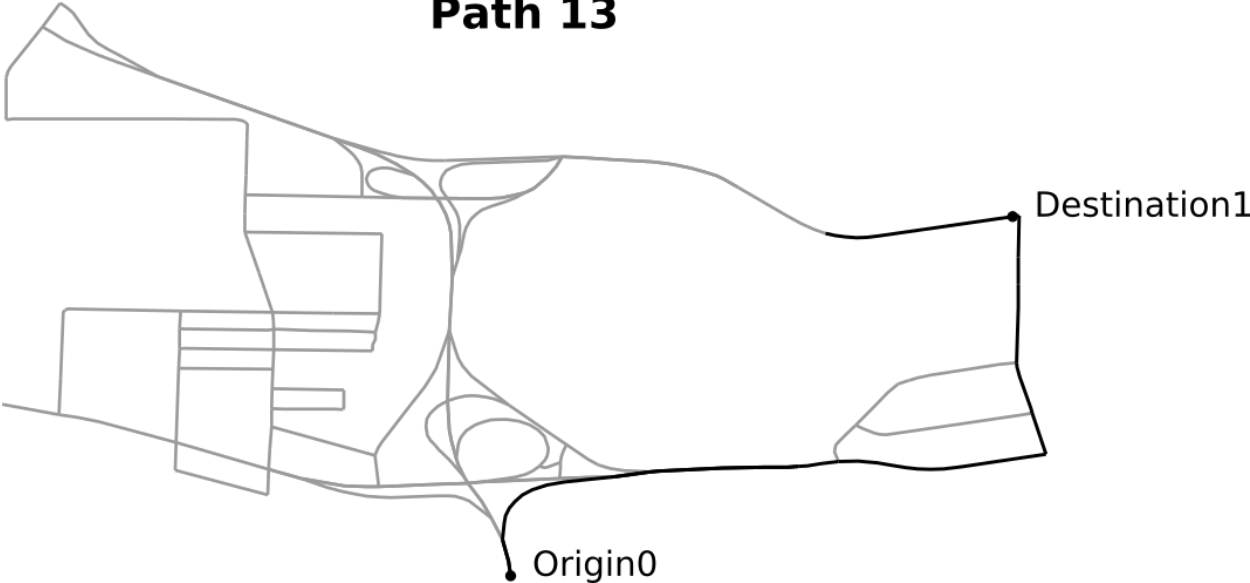


Figure D-1: Map of simplified road network in the District of North Vancouver with origin and destination points highlighted.

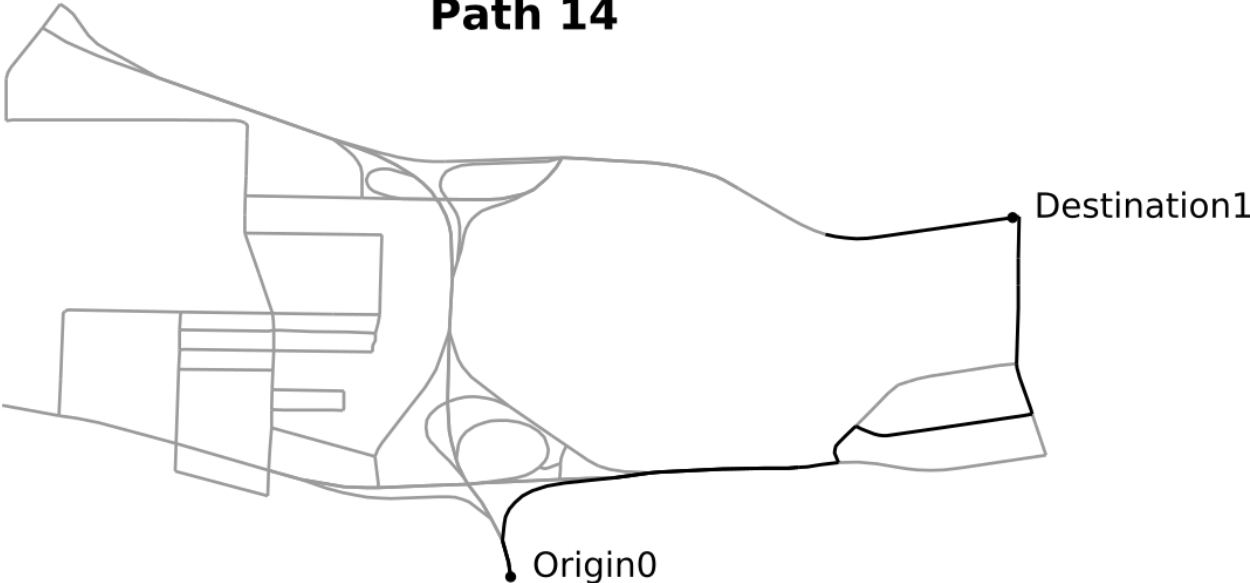
Each heading in this section identifies an origin and destination pair, and a map of each of the paths connecting the selected pair is shown. Since headings identify the points of interest, and for the sake of reducing unnecessary information and clutter, individual figure numbers are not included with the maps.

D.2 Origin 0 – Destination 1

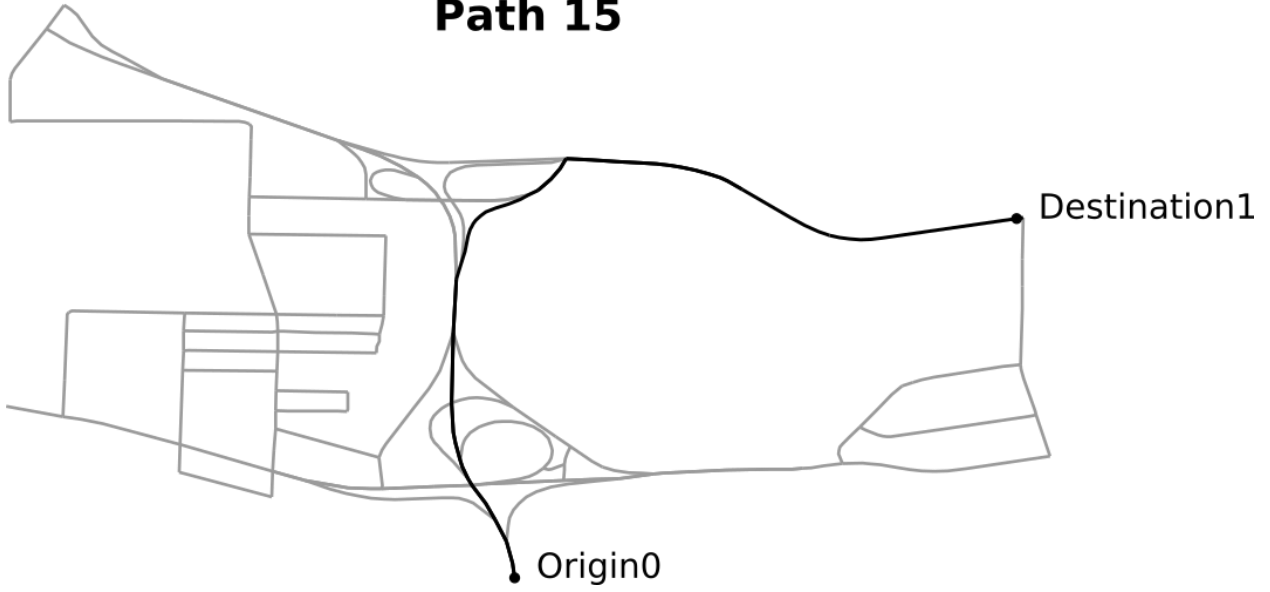
Path 13



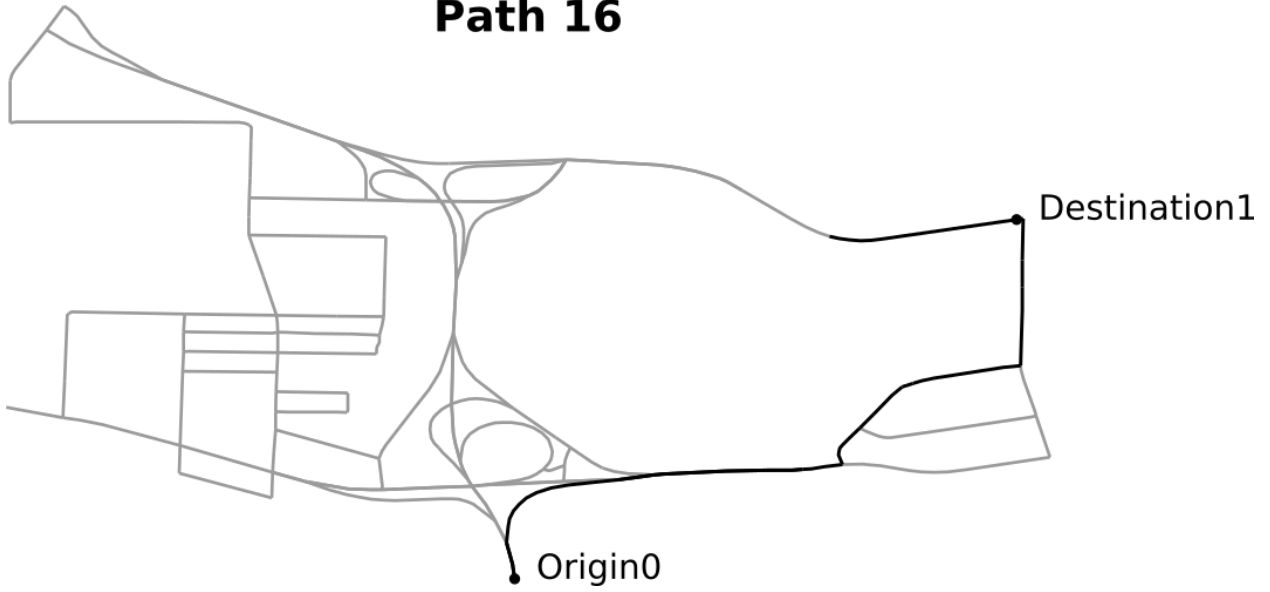
Path 14



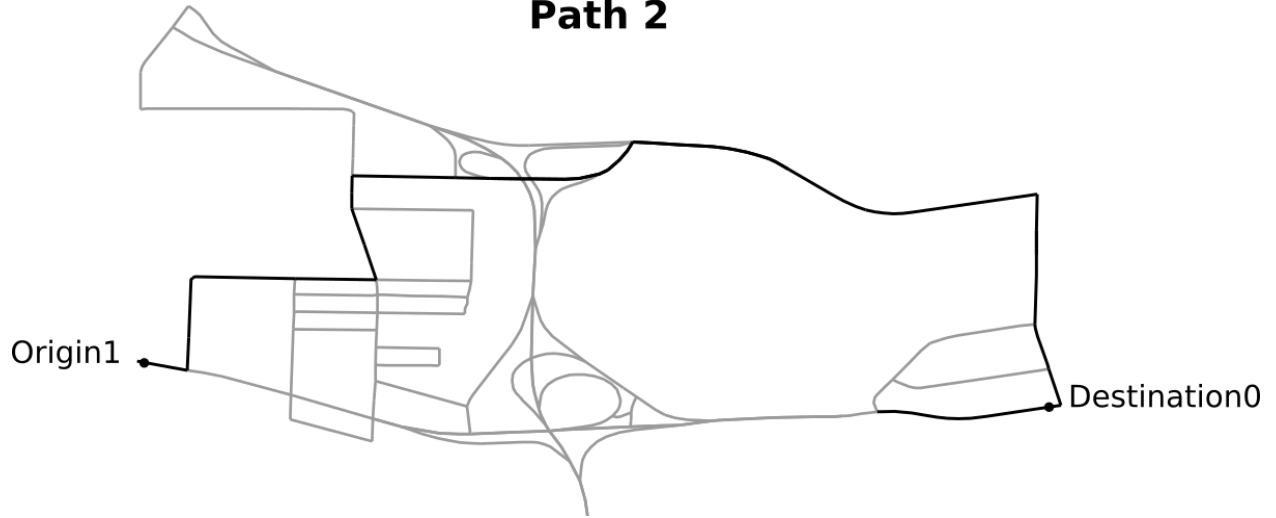
Path 15



Path 16

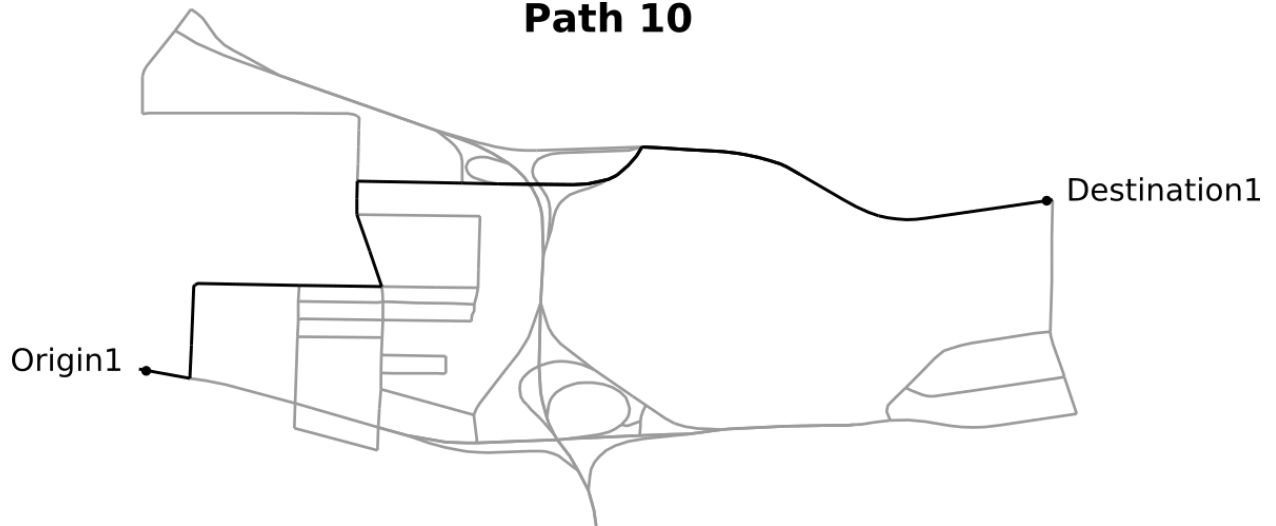


Path 2

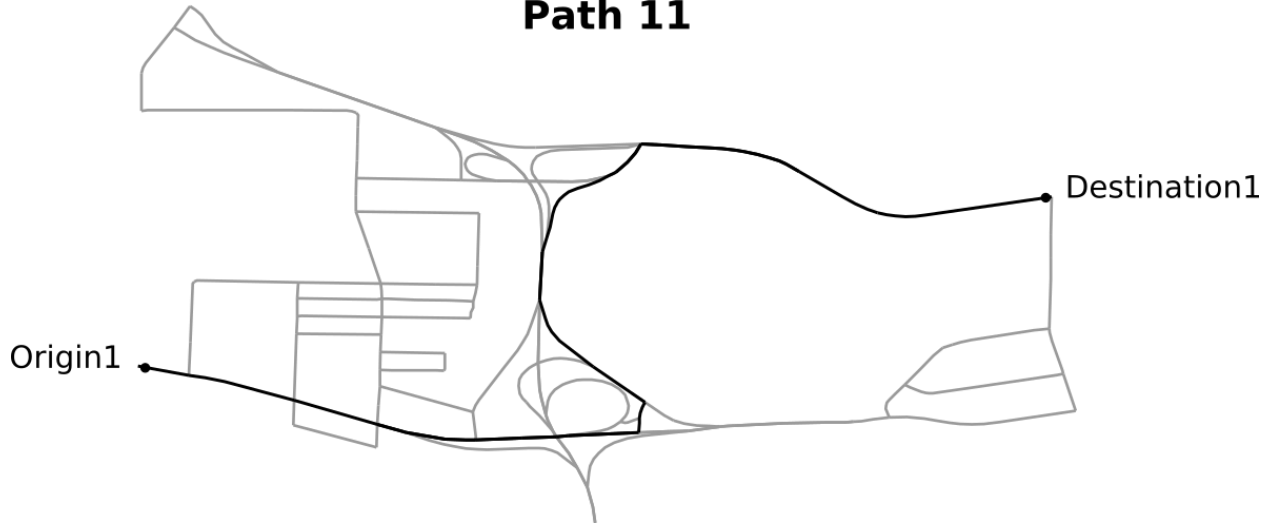


D.4 Origin 1 – Destination 1

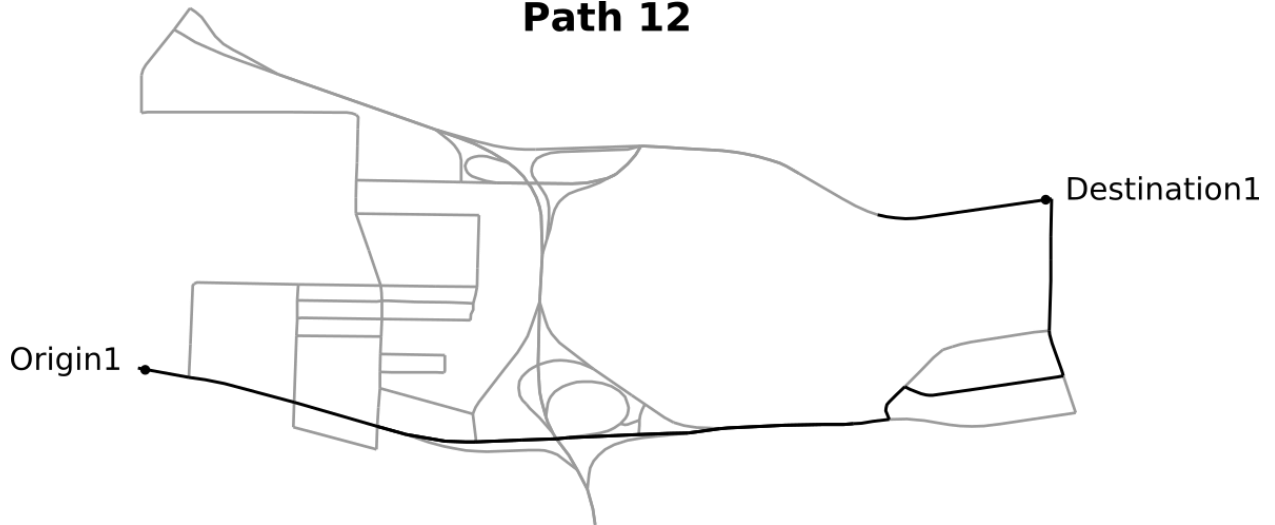
Path 10



Path 11



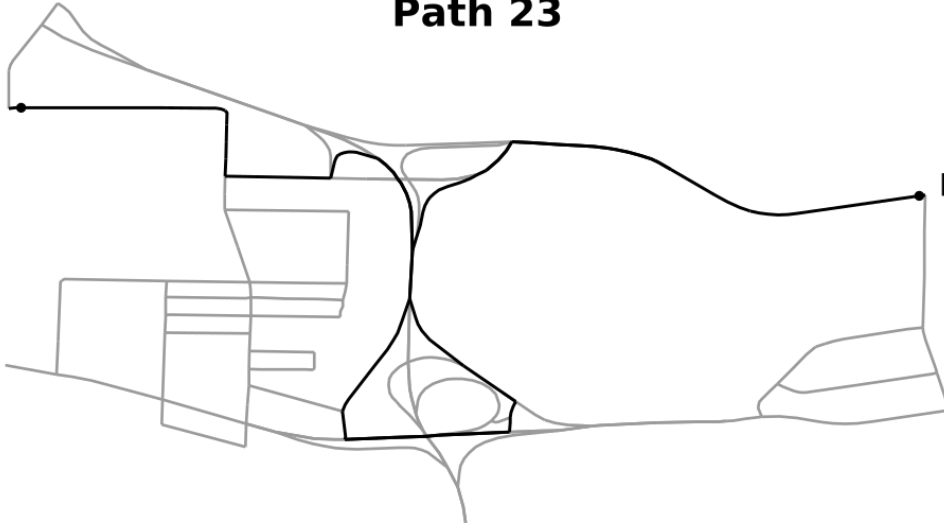
Path 12



Path 23

Origin2

Destination1



Appendix E: Box plots for performance of road networks by origin-destination pair

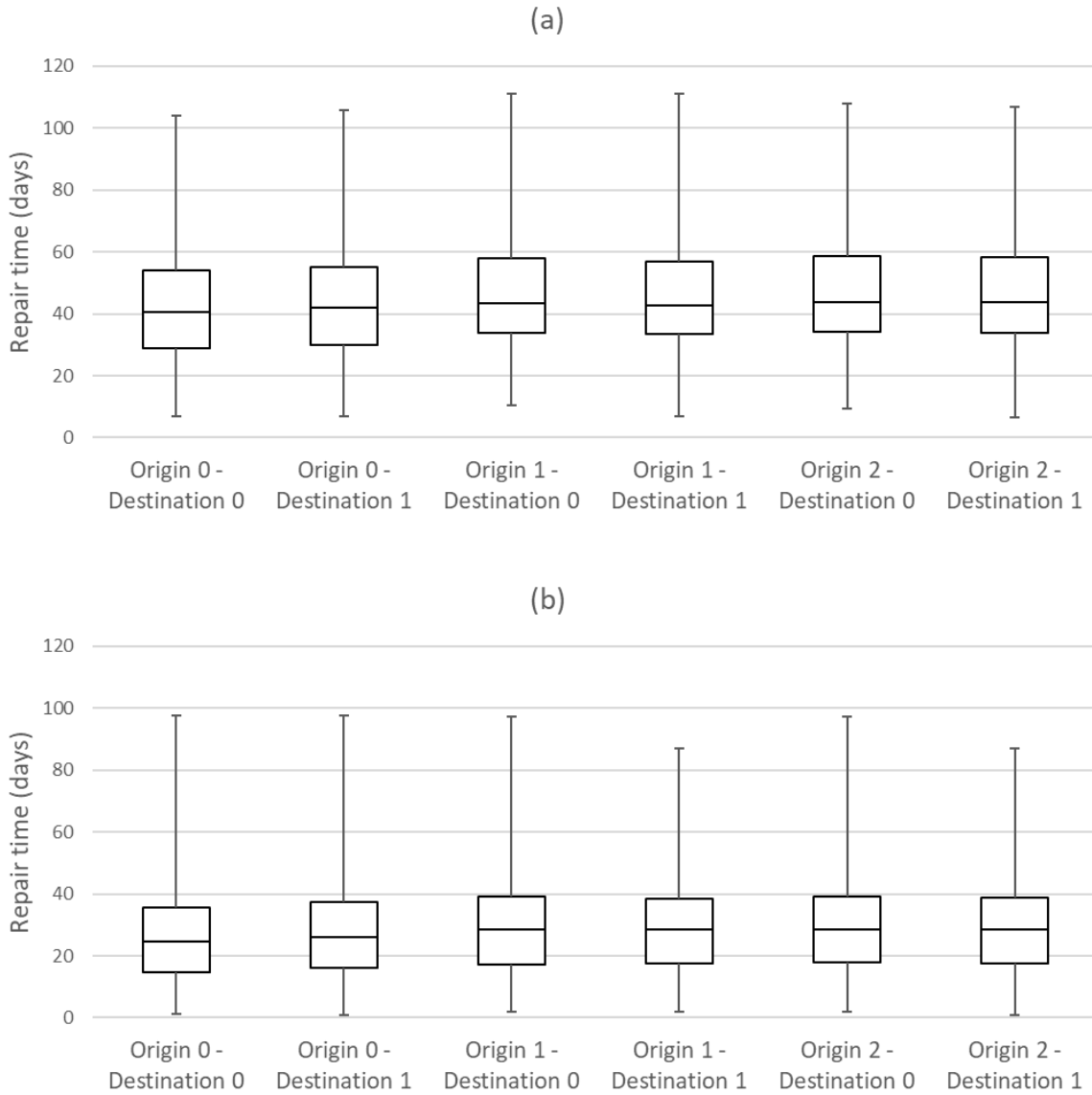


Figure E-1: Origin-destination performance for (a) randomly ordered trials; and (b) trials ordered by road importance, as defined in Section 4.4.

Appendix F: Performance of paths for randomized and ordered trials

The table below details the recovery time and standard deviation of each path (discussed in Chapter 4 and mapped in Appendix D) for randomized and ordered trials. All values are indicated in days.

	Random		Ordered	
	Mean	Standard Deviation	Mean	Standard Deviation
Path 1	46.8	18.6	30.3	15.8
Path 2	47.8	18.7	31.0	15.5
Path 3	42.7	18.3	26.8	15.3
Path 4	47.6	18.8	30.5	15.7
Path 5	47.6	18.7	30.7	15.5
Path 6	47.9	18.6	30.8	15.5
Path 7	48.2	18.6	31.0	15.6
Path 8	48.3	18.6	31.1	15.7
Path 9	48.3	18.6	31.0	15.7
Path 10	46.8	18.5	30.4	15.4
Path 11	47.2	18.6	30.6	15.8
Path 12	47.6	18.5	30.8	15.7
Path 13	46.1	18.6	29.3	15.5
Path 14	45.9	18.4	29.7	15.4
Path 15	46.7	18.7	29.8	15.8
Path 16	46.3	18.6	29.7	15.3
Path 17	47.1	18.7	30.4	15.6
Path 18	48.3	18.7	31.2	15.6
Path 19	48.3	18.7	31.2	15.6
Path 20	48.4	18.8	31.2	15.7
Path 21	48.5	18.7	31.2	15.7
Path 22	46.7	18.9	29.9	15.4
Path 23	48.1	18.6	30.9	15.6